



Neem leaf glycoprotein reverses tumor-induced and age-associated thymic involution to maintain peripheral CD8⁺ T cell pool

Ipsita Guha¹, Avishek Bhuniya¹, Partha Nandi¹, Shayani Dasgupta¹, Anirban Sarkar¹, Akata Saha¹, Juhina Das¹, Nilanjan Ganguly¹, Sarbari Ghosh¹, Tithi Ghosh¹, Madhurima Sarkar¹, Sweta Ghosh², Subrata Majumdar², Rathindranath Baral^{‡,1} & Anamika Bose^{*,‡,1}

¹Department of Immunoregulation & Immunodiagnostics, Chittaranjan National Cancer Institute (CNCI), 37, SP Mukherjee Road, Kolkata 700026, India

²Department of Molecular Medicine, Bose Institute, P1/12, CIT Scheme VIII, Kolkata 700054, India

*Author for correspondence: Tel.: +91 033 2476 5101 ext. 334; anamikabose2@gmail.com

‡Senior authors

Aim: As tumor causes atrophy in the thymus to target effector-T cells, this study is aimed to decipher the efficacy of neem leaf glycoprotein (NLGP) in tumor- and age-associated thymic atrophy. **Materials & methods:** Different thymus parameters were studied using flow cytometry, reverse transcriptase PCR and immunocyto-/histochemistry in murine melanoma and sarcoma models. **Results:** Longitudinal NLGP therapy in tumor hosts show tumor-reduction along with significant normalization of thymic alterations. NLGP downregulates intrathymic IL-10, which eventually promotes Notch1 to rescue blockade in CD25⁺CD44⁺c-Kit⁺DN2 to CD25⁺CD44⁺c-Kit⁺DN3 transition in T cell maturation and suppress Ikaros/IRF8/Pu.1 to prevent DN2-T to DC differentiation in tumor hosts. The CD5^{int}TCR $\alpha\beta$ ^{high} DP3 population was also increased to endorse CD8⁺ T cell generation. **Conclusion:** NLGP rescues tumor-induced altered thymic events to generate more effector T cells to restrain tumor.

First draft submitted: 20 September 2019; Accepted for publication: 19 June 2020; Published online: 23 July 2020

Keywords: dendritic cells • IL-10 • NLGP • thymic atrophy • thymus • tumor

The cellular immune system in the tumor microenvironment not only fails to mount an effective antitumor response, but also actively enhances the intimacy with transformed cells to promote tumorigenesis [1]. On the other hand, immunotherapy enhances altered host immune response to combat against cancer [2]. The main arsenal in both scenarios is thymus differentiated T cells. Being a site for T cell differentiation, the thymus becomes targeted in cancer, though it is known to start to involute after puberty and is believed to become nonfunctional in adults. Contrary to the traditional view, recent studies with adult thymus suggest the thymic environment is maintained throughout the life [3] and inflammatory diseases such as cancer can initiate thymopoiesis, though mainly contribute Tregs expansion rather than effector T cells [4].

In context to the tumor, several *in vivo* and *in vitro* studies with tumor-induced thymic alterations observed: alterations in thymic size and cellularity; accumulation of early CD4⁺CD8⁻ double negative (DN)-pro T cells; enhanced apoptosis of immature CD4⁺CD8⁺ double positive (DP) thymocytes; loss of CD8⁺ single positive (SP) thymocytes; alterations of thymic cytokine/chemokine gradient. All these events cumulatively diminish antitumor effector CD8⁺ T cell pool to ultimately promote impaired cellular immunity.

Neem leaf glycoprotein (NLGP) is a neem-derived natural nontoxic immunomodulator, exhibits robust anti-tumor activity, chiefly by activating CD8⁺ T cells as reported in several murine tumor models [5–7]. Corrolarily, NLGP-mediated tumor growth restriction is associated with reduction of immune-suppressor cells (regulatory T cells, tumor-associated macrophages, myeloid-derived suppressor cells and dendritic cells) [8–11] and vascular

angiogenesis [12]. In this context, it is of interest to study the impact of NLGP immunotherapy in modulation of intra-thymic T cell differentiation and maturation process, which is dampened in tumor host.

Thymic atrophy is defined as shrinkage of thymus, which results in smaller thymus size and reduced cell number [13–15]. Herein, we report that, NLGP immunotherapy can reduce tumor-induced thymic involution in both young and elderly tumor hosts by maintaining thymic weight, volume and cellularity. NLGP normalizes the cytokine microenvironment by downregulating intrathymic IL-10 to ensure proper T cell lineage commitment through DN-DP-SP stages of T cell differentiation, possibly by promoting optimum interaction between thymic stromal cells and thymocytes by regulating several transcription factors.

Materials & methods

Antibodies & reagents

Anti-mouse biotin conjugated antibodies (biotin conjugated-lineage cocktail and Thy1.2); antimouse fluorescence conjugated antibodies (FITC conjugated CD4, CD8, CD44 and MHCII; PE conjugated CD25 and CD11c; PerCP cy5.5 conjugated c-Kit) and CytoFix/CytoPerm solution was procured from BD Pharmingen (CA, USA). Purified anti-mouse antibodies (CD4, CD8, CD45, Ikaros and Notch1) were purchased from Biolegend (CA, USA).

Neem leaf glycoprotein

From neem (*Azadirachta indica*) leaves, NLGP was prepared by the method as described previously [16,17]. Matured neem leaves of same size and color were collected, shed dried and pulverized. Leaf powder was soaked overnight in phosphate-buffered saline (PBS), pH 7.4. Then supernatant was collected by centrifugation at 1500 r.p.m. and dialyzed against PBS. After that this supernatant was concentrated by centricon membrane filter (Millipore Corporation, MA, USA) with 10 kDa molecular weight cut-off (maximum tumor restricting activity is obtained when it was concentrated by using 10 kDa cut-off membrane). Purity of NLGP in each batch was checked by size-exclusion HPLC (SE-HPLC) and PAGE analysis [5,6,18,19]. The protein concentration was measured by Lowry's method and its functionality was validated by tumor growth restriction assay as described [5,6].

Mice & tumor

Swiss and C57BL/6 mice (age, 4–6 weeks and 6/8 months; body weight, 20–25 and 30–32 g on average) were obtained from Animal Facilities of the National Institute of Nutrition, Hyderabad, India. The care and treatment of animals conformed to guidelines established by the Institutional Animal Care and Ethics Committee. Autoclaved dry pellet (Epic Laboratory Animal Feed, Kalyani, India) and water were given *ad libitum*. Mice were housed in pathogen-free environment. The study was approved by Institutional Animal Care and Ethics Committee (Approval No. IAEC-1774/RB-4/2015/6, IAEC-1774/RB-4(Ext)/2017/5 and IAEC-1774/RB-19/2017/15). Mice were inoculated with Sarcoma 180 and B16 melanoma tumor cells subcutaneously to Swiss and C57BL/6 mice respectively in the lower flank.

Tumor growth measurement & NLGP injection

Three groups (normal, tumor and tumor + NLGP) of Swiss mice (n = 6 in each group) were inoculated with sarcoma (1×10^6 cells/mice) and B16 melanoma (2×10^5 cells/mice) in the lower right flank to develop solid tumor, and tumor growth was monitored biweekly by caliper measurement using the formula: (length \times width). Tumor size was recorded as tumor area (in mm²) and mice were sacrificed if tumors became ulcerated or reached a size of 20 mm in either direction. The protocols conformed to guidelines established by the Institutional Animal Care and Ethics Committee. Palpable tumor was observed after 7–10 days. Then NLGP (25 μ g/100 μ l PBS/mice) subcutaneously was given in left hind leg of mice for 3 weeks with 7 days interval.

RT-PCR

Cellular RNA was isolated using Trizol (Invitrogen, CA, USA) and random hexamers were used to generate corresponding cDNA (First Strand cDNA Synthesis Kit; Fermentas, MD, USA). Amplification was performed using 2X Go Taq Green Mix (Promega, WI, USA) and PCR was carried out with gene-specific primer listed in Table 1 with the following program: 94°C for 5 min; 35 cycles of 94°C for 30 s, 54–57°C for 30 s and 72°C for 1 min; and 72°C for 5 min. PCR products were identified by image analysis software for gel documentation (Versadoc; BioRad Laboratories, CA, USA) after electrophoresis on 1.5% agarose gels and staining with ethidium

Table 1. Primer list.

Gene	Accession n	Primer sequence (5'-3')	Product length
<i>β-actin</i>	NM.007393.5	Forward: 5'-CAACCGTGAAAAGATGACCC-3' Reverse: 5'-ATGAGGTAGTCTGTCAAGTC-3'	228 bp
<i>il-2</i>	NM.008366.3	Forward: 5'-GCAGGCCACAGAATTGAAAG-3' Reverse: 5'-TCCACCACAGTTGCTGGACTC-3'	207 bp
<i>il-2r</i>	NM.008368.4	Forward: 5'-GACTGAATGCAGCCTGTTGA-3' Reverse: 5'-GGTCCCCAAGCAACATAGA-3'	228 bp
<i>il-4</i>	NM.021283.2	Forward: 5'-CCAGCTAGTTGTCATCCTGCTTCTTCTCG-3' Reverse: 5'-CAGTGATGTGGACTTGGACTCATTGATGGTGC-3'	358 bp
<i>il-6</i>	NM.031168.2	Forward: 5'-TTCATCCAGTTGCCTTCTT-3' Reverse: 5'-CAGAATTGCCATTGCACAAC-3'	199 bp
<i>il-7</i>	NM.001313888.1	Forward: 5'-TGAGTGCCACATTAAGACA-3' Reverse: 5'-AAGCAGCTTCCTTTGTATCA-3'	161 bp
<i>il-10</i>	NM.010548.2	Forward: 5'-CCAAGCCTTATCGGAAATGA-3' Reverse: 5'-TTTTACAGGGGAGAAATCG-3'	162 bp
<i>ccl 17</i>	NM.011332.3	Forward: 5'-ATGAGGTCACCTCAGATGCT-3' Reverse: 5'-AGCTCACCAACTTCTGATA-3'	148 bp
<i>ccl 19</i>	NM.011888.2	Forward: 5'-GCTAATGATGCGGAAGACA-3' Reverse: 5'-ACTTCTCAGTCTTCGGATG-3'	199 bp
<i>ccl 21</i>	NM.011124.4	Forward: 5'-AAGTTTAGGCTGTCCATCC-3' Reverse: 5'-TTAGAGTTCCCGGTTCTT-3'	174 bp
<i>cxcl 12</i>	NM.021704.3	Forward: 5'-CTGCATCAGTGACGGTAAACC-3' Reverse: 5'-CAGCCGTGCAACAATCTGAAG-3'	142 bp
<i>ccr 9</i>	NM.001166625.1	Forward: 5'-ATTCTTGAGTCAGGCTGT-3' Reverse: 5'-AAGTACCCTCTCTCCTTGT-3'	242 bp
<i>ccr 7</i>	NM.001301713.1	Forward: 5'-GTGTGCTCAAGAAGGATGT-3' Reverse: 5'-GAAGGGAAGAATTAGGAGGA-3'	201 bp
<i>cxcr 4</i>	NM.009911.3	Forward: 5'-TCAGTGGCTGACCTCCTCTT-3' Reverse: 5'-CTTGGCCTCTGACTTGGGT-3'	203 bp
<i>ccr 4</i>	NM.009916.2	Forward: 5'-GCTCCTCTTACACGCACTCC-3' Reverse: 5'-CTTGCCATGGTCTTGTTTT-3'	180 bp
<i>notch 1</i>	NM.008714.3	Forward: 5'-CTCAATGGGTACAAGTGTGA-3' Reverse: 5'-TGATGTTGGTCTGGCAATTA-3'	178 bp
<i>tcf 1</i>	NM.009327.3	Forward: 5'-GAAGCCAGTCATCAAGAAAC-3' Reverse: 5'-TAGACTTGGCTGCTCTTC-3'	162 bp
<i>pax 5</i>	NM.008782.3	Forward: 5'-CATCAAGCCAGAACAGACCA-3' Reverse: 5'-AAGTCTCGGCCTGTGACAAT-3'	156 bp
<i>bcl11b</i>	NM.001079883.1	Forward: 5'-GAGCACAGAAGAAACAGTG-3' Reverse: 5'-GACAGTAGGTGGTCATCTTG-3'	161 bp
<i>ikaros</i>	NM.001301868.1	Forward: 5'-GGAAGAAAATAACCAACAACG-3' Reverse: 5'-TCCTTCTCATAGTTGGCACT-3'	180 bp
<i>irf 4</i>	NM.001347508.1	Forward: 5'-GGCATTGTTAAAGGCAAGT3' Reverse: 5'-GTGTCATCAAAGTGAGCTG 3'	210 bp
<i>irf 8</i>	NM.001301811.1	Forward: 5'-GAAGACCATGTTCCGTATCC-3' Reverse: 5'-AAATCTGGGCTCTTGTTCAG-3'	180 bp
<i>relb</i>	NM.001290457.1	Forward: 5'-TTCTCCCTGCTTCCATATC-3' Reverse: 5'-CAGGTCCAACATAGTGAAGA-3'	117 bp
<i>pu.1</i>	NM.019866.1	Forward: 5'-CCTTCGATCCTGCTACTGCT-3' Reverse: 5'-CAGGTCCAACATAGTGAAGA-3'	176 bp
<i>il-7r</i>	NM.001355680	Forward: 5'-CCACAATGAGTGCCCTACCT-3' Reverse: 5'-GACCGGACAGACTCCAAT-3'	238 bp
<i>il-15</i>	NM.010548.2	Forward: 5'-ATCTCGTGACTTGTGTTT-3' Reverse: 5'-GTAATTTGCAACTGGGATG-3'	221 bp
<i>il-10r</i>	NM.008348.3	Forward: 5'-GTCTCAAGGGATGGCTTCTG-3' Reverse: 5'-GCCGCTGTCATTCTTACC-3'	245 bp

bromide (Sigma-Aldrich, MO, USA). Reverse transcriptase PCR primers were designed and purchased from MWG-Biotech (Bangalore, India) [20].

Flow-cytometric staining

Thymocytes were isolated from normal and tumor hosts with or without NLGP treatment. Lineage negative Thy1.2 positive population was obtained by removal of mature lineage positive cells using the following cocktails of biotinylated lineage antibodies: anti-B220, anti-TER119, anti-CD11b (Mac-1), anti-Gr-1, anti-CD3e (Biolegend), followed by negative selection using by BD IMag streptavidin particles-DM (BD Biosciences, CA, USA); and Thy1.2-positive cells were isolated by positive selection using BD IMag anti-mouse Thy1.2 (CD 90.2) biotin streptavidin particles-DM (Biolegend), then those cells were sorted based on CD44 and CD25 expression using a FACSAria cell sorter (Becton Dickinson, CA, USA). Flow-cytometry was used to determine cell-surface phenotypes after first staining cells (1×10^6) with fluorescently labeled antibodies (specific and isotype-matched controls). After incubation for 30 min at 4°C in the dark, labeled cells were washed twice with FACS buffer (0.1% bovine serum albumin [BSA] in PBS) before flow-cytometric analysis. Similarly, intracellular molecules (i.e., Notch1 and Ikaros) were stained with anti-mouse fluorescence-labeled antibodies using Cytofix/Cytoperm reagents per the manufacturer's protocol (BD Biosciences). Cells were then fixed with 1% paraformaldehyde in PBS; acquisition was performed using a FACS Calibur (Becton Dickinson) along with suitable negative isotype controls. The percentage of positively stained populations was determined using quadrant statistics established using Cell Quest (Becton Dickinson) and FlowJo software (Tree Star, OR, USA) [20].

Histopathology of thymus section

Thymus tissue samples were harvested and embedded in paraffin to prepare blocks. Samples were frozen for cryosection. From the tissue block 5- μ m sections were stained with haematoxyline and eosin as previously reported [12]. Sections were immunostained by CD11c by the protocol reported earlier [7]. Imaging was performed under bright field microscope (Carl Zeiss, Jena, Germany).

Fluorescence imaging of thymus sections

Cryo-sectioned thymus tissue samples were stained as previously reported [21]. FITC-conjugated antimouse CD44 and PE-conjugated anti-CD25 or matching isotype controls were used for fluorescence staining. Imaging was performed under fluorescence microscope (Olympus BX53, Tokyo, Japan) and analyzed using ImageJ software (<https://imagej.net/Fiji>).

Statistical analysis

All reported results represent the mean \pm standard error of mean (SEM) of data obtained in six (for *in vivo* analysis) independent experiments. Statistical significance was established by unpaired *t*-test and one-way analysis of variance (ANOVA) using INSTAT3 Software (Graphpad, CA, USA) by Turkey's multiple comparison with differences between groups attaining a p-value 0.05 considered as significant.

Results

NLGP normalizes tumor influenced thymic alteration

In agreement with earlier reports [22,23] we observed that tumor progression promotes severe thymic alterations, in other words, thymic weight and cell numbers were decreased significantly with increased tumor size (Figure 1Ai); perivascular spaces were increased and cortex to medulla ratio became downregulated in comparison to normal. Moderate decrease in thymic weight, volume and cellularity was noticed in initial phase of tumor growth (tumor area: 70–80 mm²), however, with progression of tumorigenesis (tumor area: 270–290 mm²), these changes become more prominent. In view of the robust immunomodulation of NLGP in restricting the murine tumor growth as well as in normalization of the altered immune functions [5,12,24,25] we have explored the effect of NLGP on these tumor-influenced thymic functions. Here, we have observed that NLGP therapy normalized thymic weight, volume and cell number, along with restriction of the murine tumor growth (Figure 1Aii). In general, thymic cortex to medulla ratio is 2:1 (two cortices to the medulla) [26], but it get altered in the thymus from tumor host from 2:1 to 1:1. Interestingly, NLGP treatment reverses the decreased cortex medulla ratio toward normalcy (Figure 1B). On the other hand, perivascular space (transit pathway for progenitor cells to immigrate into the thymus) also get

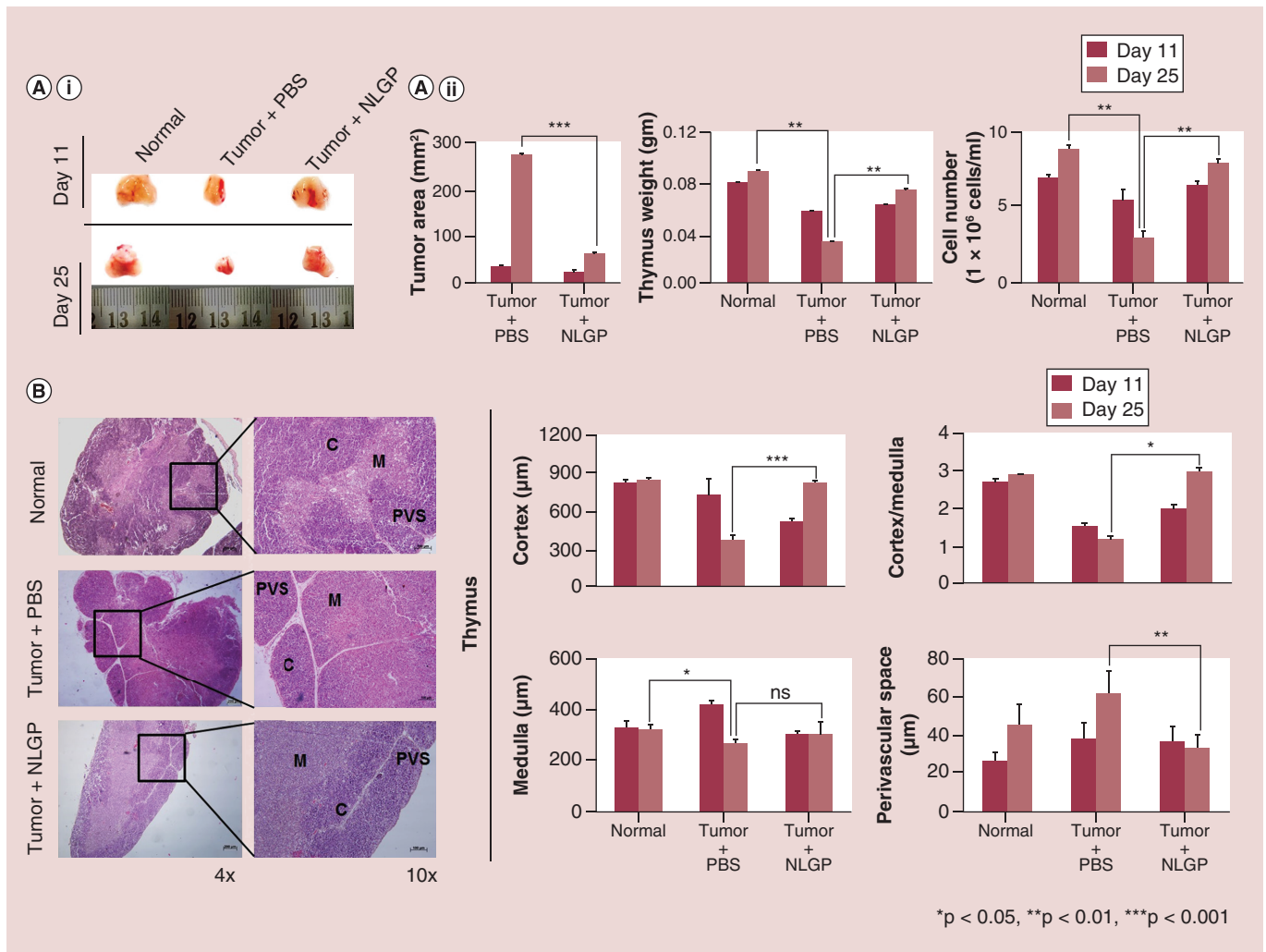


Figure 1. Neem leaf glycoprotein normalizes tumor induced thymic alterations. (Ai) Representative figures of thymus from normal, tumor + PBS and tumor + NLGP cohorts on day 11 and 25 following tumor inoculation, n = 6 in each case. **(Aii)** Bar diagrammatic representation of mean ± SEM of tumor area (mm²), thymus weight (gm) and thymic cell number (1 × 10⁶ cells/ml) from normal, tumor + PBS and tumor + NLGP hosts on day 11 and 25, n = 6 in each group. **(B)** Histopathology of cortex, medulla and PVS from three different cohorts was identified by haematoxyline and eosin staining; 4× and 10× insets are shown. Bar diagrammatic representation of mean ± SEM of cortex (µm), medulla (µm) and cortex:medulla ratio and PVS (µm) of thymus from normal, tumor + PBS and tumor + NLGP hosts on day 11 and 25, (n = 6, in each cohort), *p < 0.05, **p < 0.01, ***p < 0.001. NLGP: Neem leaf glycoprotein; PBS: Phosphate-buffered saline; PVS: Perivascular space.

increased in tumor host, however, increased perivascular space surrounding blood vessels get reduced after NLGP treatment (Figure 1B).

NLGP modulates thymic cytokine–chemokine microenvironment

Thymic cytokines and chemokines co-ordinately modulate T cell differentiation and maturation process by regulating proper (pro-T cell) T cell migration and its sequential interaction with stromal cells [27,28]. Given the ability of NLGP in ensuring normalization of tumor induced thymic alteration in comparison to normal thymus, we aimed to investigate the influence of NLGP in thymic cytokine-chemokine microenvironment of tumor host. Tumor burden alters normal expression of cytokines [29]. Reduced expression of *il-7* along with increase in *il-10* and *il-6* expressions (Figure 2A) were noted in thymus of tumor bearing mice. However, in NLGP treated mice *il-7* expression in mRNA level was increased. On the other hand, expression of *il-10* was significantly reduced along with moderate reduction in expression of *il-6* in thymus of NLGP treated tumor-bearing mice (Figure 2A). In view of the significant decrease of *il-10* in thymus, we opted for immunohistochemical study of IL-10 in thymus

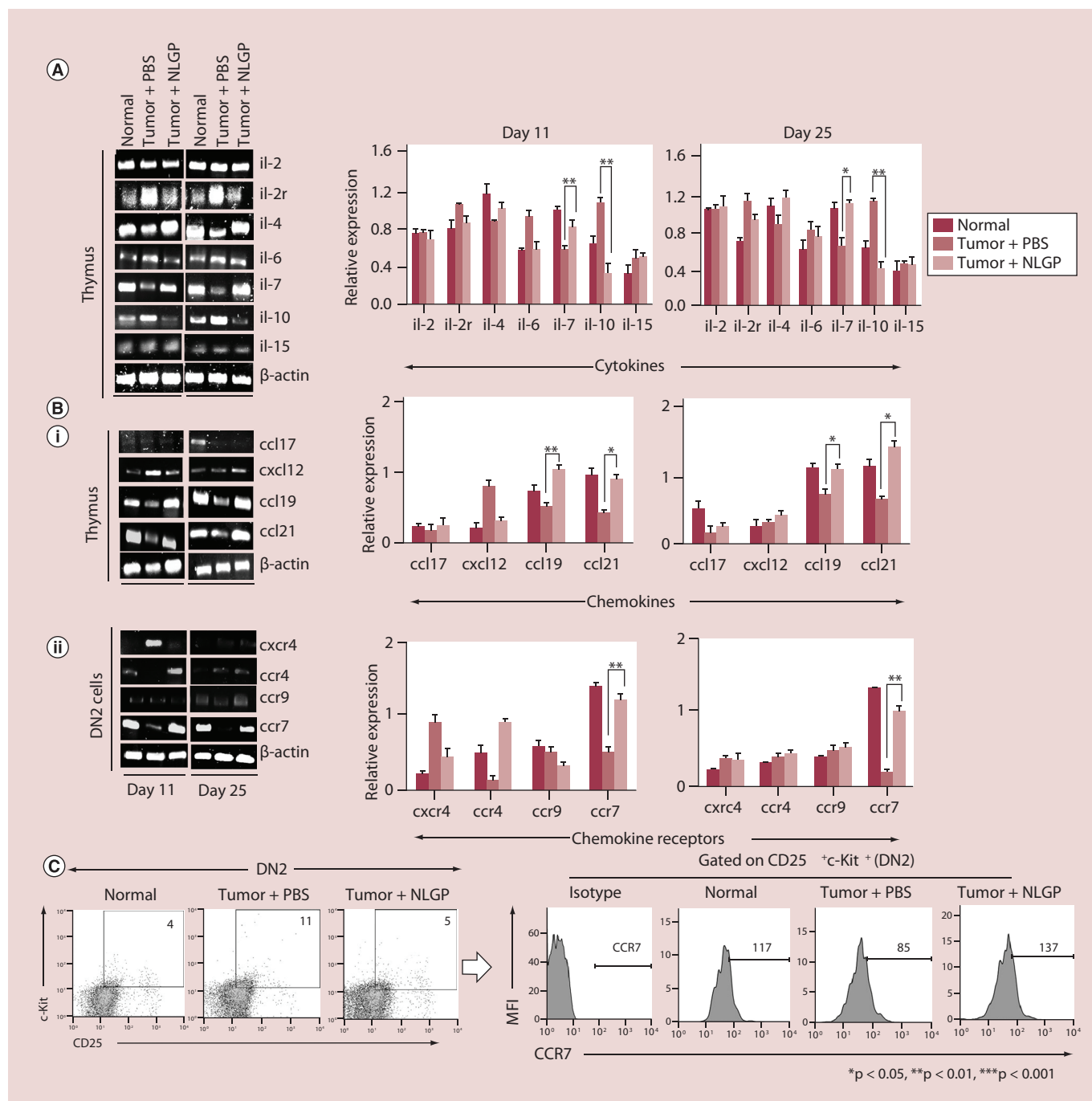


Figure 2. Neem leaf glycoprotein rectifies altered thymic cytokine–chemokine microenvironment. Total thymic mRNA was isolated from three mice cohorts (normal, tumor + PBS and tumor + NLGP) ($n = 4$, in each cohort) and assessed by RT-PCR, keeping β -actin as a loading control for gene expression of cytokines (A), chemokines (Bi) and chemokine receptors (Bii) on day 11 and 25 following tumor inoculation. Cytokines like *il-2*, *il-2r*, *il-4*, *il-6*, *il-7*, *il-10* and *il-15*; chemokine ligands, like *ccl17*, *cxcl12*, *ccl19*, *ccl21* and chemokine receptors, like *cxcr4*, *ccr4*, *ccr9* and *ccr7* were studied at gene level. Representative figures are shown in left panel, along with bar diagram of mean \pm SEM of gene expression from normal, tumor + PBS and tumor + NLGP hosts on day 11 and 25, * $p < 0.05$, ** $p < 0.01$, *** $p < 0.001$. (C) Flow-cytometric dot plot analysis of CD25⁺c-Kit⁺ thymic cells from normal, tumor + PBS and tumor + NLGP mice groups. Representative histogram figures for CCR7 on CD25⁺c-Kit⁺ (DN2) gated cells, (mean \pm SEM); $n = 4$. NLGP: Neem leaf glycoprotein.

sections of mice from different treatment cohorts and results showed the increased IL-10 expression in thymic sections from tumor host that get significantly reduced in thymus from NLGP treated mice (data not shown).

In view of the documentation of role of chemokine receptors and their corresponding ligands in the migration of immature cells and emigration of mature cells from thymus [30,31], the chemokine ligands and receptors were studied precisely. Study of several chemokine ligands in total thymic cell population revealed a significant decrease of *ccl19* and *ccl21* (ligands for CCR7) in thymus from tumor-bearing mice, which was normalized following NLGP treatment (Figure 2Bi). However, no significant alteration was observed in *ccl17* (ligand for CCR4) and *cxcl12* (ligand for CXCR4) in thymus from tumor host with or without NLGP treatment. Considering the significant changes in *ccr7* ligands, next we analyzed CCR7 expression in flow-sorted DN2 subpopulations isolated from tumor bearing mice in comparison to those having NLGP treatment, as CCR7 expression on DN2 facilitates its migration from CMJ to subcapsular region for maturation [32]. CCR7 expression was found to be severely impaired in DN2 subpopulation of tumor host, while DN2 isolated from NLGP treated tumor bearing mice showed almost normalized level of expression required for DN2-pro T cell migration from cortex to sub-capsular region (Figure 2Bii). Flow-cytometric analysis also validates normalization of the CCR7 from 17% to 28% in NLGP treated cohort (Figure 2C).

NLGP efficiently promotes T cell commitment by differentially regulating Notch1 & Ikaros signaling

During normal thymopoiesis DN pro-T cells with multi-lineage potential progress toward T cell lineage commitment through different maturation steps: DN1 (CD25⁻CD44⁺), DN2 (CD25⁺CD44⁺), DN3 (CD25⁺CD44⁻) and DN4 (CD25⁻CD44⁻) under the direct control of several transcription factors [33]. Recently, we have observed a significant arrest in DN2 to DN3 transition with a diversion of these DN2 toward thymic dendritic cells (DCs) in tumor host [20]. Interestingly, we observed that NLGP immunotherapy in tumor host can direct DN2 cell differentiation toward maturation with normalization of DN2 (Figure 3A). Immunofluorescence study also revealed a decrease of CD44 and CD25 colocalization in cortico medullary junction (CMJ) region suggesting a NLGP-mediated downregulation of tumor-associated DN2 accumulation in thymus (Figure 3Bi). DN2 cells were further studied by analyzing DN2a (CD25⁺CD44⁺c-Kit^{high}) and DN2b (CD25⁺CD44⁺c-Kit^{low}) pro-T cells by flow-cytometry in thymus from tumor host with or without NLGP treatment and results revealed abundance of DN2b pro-T cells in tumor host get significantly normalized within NLGP-treated cohort (Figure 3Bii).

Considering the importance of transcription factors in T cell maturation [34], we have checked *notch1*, *ikaros*, *pu.1*, *bcl11b* and *irf8* etc in sorted DN2 cells from both cohorts. Decreased *notch1* expression in DN2 cells from tumor host was significantly enhanced in NLGP treated tumor bearing mice, with decreased expression of *ikaros*, *Pu.1* and *irf8* (Figure 3C). In line of the upregulated *notch1* expression in thymus after NLGP treatment, we also found sustained expression of *bcl11b* in same cohort, which may further promote T cell maturation [35,36]. Moderate alteration was found in other lineage determinant transcription factor like *pax5* (for B-cell lineage) and *pu1.1* (for macrophage lineage) in thymus of untreated or NLGP treated tumor bearing mice (Figure 3C). As Ikaros, PU.1 and IRF8 are responsible for dendritic cell lineage commitment, further we analyzed the frequency of CD45⁺MHCII⁺CD11c⁺ cells by flow-cytometry in thymus from both cohorts. Increased frequency of CD45⁺MHCII⁺CD11c⁺ cells in tumor thymus are decreased (28% to 8%) by NLGP treatment (Figure 3Di). The observation was supported by immunohistochemistry where decreased frequency of CD11c⁺ cells in thymic tissues from NLGP treated tumor-bearing mice (Figure 3Dii) was noted in comparison to untreated tumor host.

NLGP selectively promotes DP to CD8⁺ SP T cell differentiation in tumor host

Blockage of DN2 to DN3 transition in the thymus of tumor host results declined output of CD4⁺ and CD8⁺ T cells in circulation thereby abrogating immune efficacy [37]. To examine this hypothesis, we wanted to know the status of DP and SP T cells in thymus of tumor-bearing mice with or without NLGP treatment. First, various subgroups of CD4⁺CD8⁺ (DP) cells, in other words, DP1 (CD5^{low}TCRαβ^{low}), DP2 (CD5^{high}TCRαβ^{int}) and DP3 (CD5^{int}TCRαβ^{high}) cells were checked by flow cytometry (Figure 4A). Results suggest significant decrease in DP cells of various categories in the thymus from tumor host. However, following NLGP treatment such DP cells, particularly CD4⁺CD8⁺CD5^{int}TCRαβ^{high} (DP3) population, were increased significantly (Figure 4A). As a consequence of elevation of DP3 population, a significant increase in CD8⁺ T cells (SP) was observed in thymus along with expanded CD8⁺ T cells in blood, lymph node and spleen in NLGP-treated tumor-bearing mice (Figure 4Bi-iv). We also checked the CD4⁺ T cells in thymus and other immune organs from tumor host with or without NLGP therapy. However, no noticeable change in CD4⁺ T cells was detected following NLGP treatment.

NLGP normalizes tumor-induced thymic involution in elderly tumor host

Similar to the pathological thymic involution in tumor host, thymic involution is also seen in elderly individuals. To ascertain whether NLGP immunotherapy can rescue the age related thymic alteration, a brief experimentation was performed in elderly mice (6 and 8 months old) with or without tumor load, but having NLGP immunotherapy. Thymus size and weight were reduced in elderly mice compared with young mice and such a reduction was more prominent in tumor-bearing elderly mice (Figure 5Ai, Aii & Aiii). Interestingly, NLGP partially reverses the situation in both cases. DN to DP arrest as observed in tumor-bearing mice was also found in elderly tumor host. In both cases, NLGP reverses the situation by potentiating the movement of pro-T cells toward DP (Figure 5Bi, Bii, Biii & Biv, Supplementary Figure 1). However, effect of NLGP was more prominent in young tumor-bearing mice than elderly. In elderly mice also, NLGP treatment caused more number of CD8⁺ T cells in circulation that was correlated well with tumor growth restriction in tumor hosts of 6 and 8 month age old (Figure 5Bv-vii;

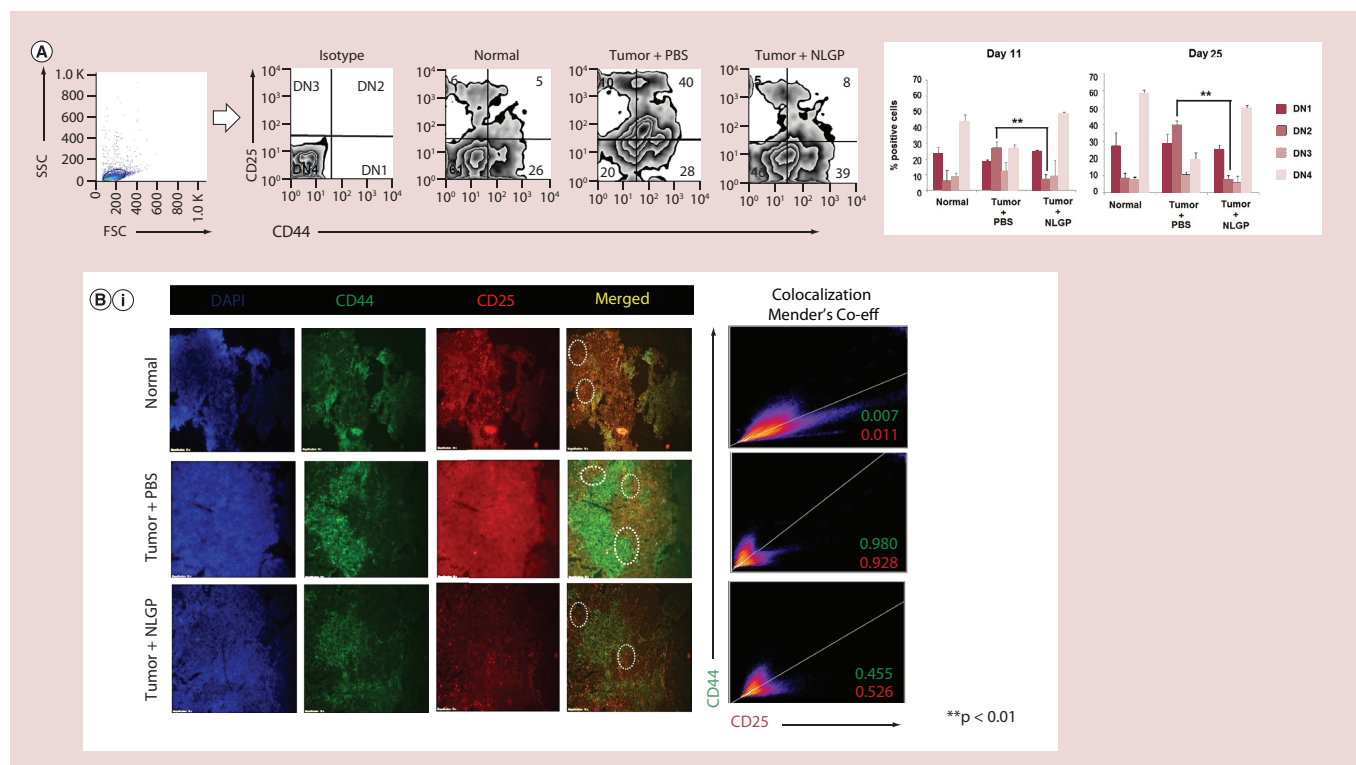


Figure 3. Neem leaf glycoprotein promotes T cell commitment by differentially regulating Notch1 and Ikaros signaling.

(A) Flow-cytometric analysis of thymic T cells based on CD25 and CD44 representing DN1 to DN4 T cells of normal, tumor + PBS and tumor + NLGP mice cohorts. Bar diagrammatic representation shows mean ± SEM of positive percentage of DN1 (CD25⁺CD44⁺), DN2 (CD25⁺CD44⁺), DN3 (CD25⁺CD44⁻) and DN4 (CD25⁻CD44⁺) T cells from above mentioned mice groups. (Bi) Immunofluorescence staining with CD25-PE and CD44-FITC was performed in thymuses from normal, tumor + PBS and tumor + NLGP hosts. Representative merged figure of stained tissues show the co-localization of CD25 and CD44 and dotted circles indicate the CD44⁺CD25⁺ localized regions. Representative 2D intensity histogram shows colocalization of CD25 and CD44; Manders' co-efficient represents the intensity and index of colocalization. Value close to 1 indicates reliable colocalization, (n = 4 in each case). (Bii) Flow-cytometric representation of thymic T cells with CD25, CD44 and c-Kit staining represent the percentage of DN2a and DN2b cells. Bar diagrammatic representation of positive percentage of DN2a (CD25⁺CD44⁺c-Kit^{high}) and DN2b (CD25⁺CD44⁺c-Kit^{low}) cells from normal, tumor + PBS and tumor + NLGP mice groups (mean ± SEM), n = 4, p-values are indicated in corresponding figures. (Biii) Thymic T cells were flow-cytometrically sorted for CD25⁺CD44⁺ as DN2 and DN3 respectively from normal, tumor + PBS and tumor + NLGP mice cohorts on day 11 and 25 after tumor inoculation. Using isolated mRNAs, different gene expressions were checked by RT-PCR, keeping β-actin as a loading control. *notch1* and *tcf1*, for T cell lineage; *pax5* for B cell lineage and *pu.1*, *ikaros*, *irf8*, *irf4* and *relb* for myeloid lineage commitment were checked. (Biv) Thymic cells were stained with CD45, CD11c and MHCII. Dot plot representation of CD45⁺CD11c⁺MHCII⁺ reveals the number of total dendritic cells. Bar diagram represents mean ± SEM of percent positive cells of CD45⁺CD11c⁺MHCII⁺ population assessed by flow-cytometry from above mentioned mice groups, (n = 3 in each groups); ***p < 0.001. (Bv) CD11c rich regions were identified immunohistochemically in thymus from normal, tumor + PBS and tumor + NLGP mice cohorts and shown in 10x, 20x and 40x magnifications.

NLGP: Neem leaf glycoprotein; PBS: Phosphate-buffered saline.

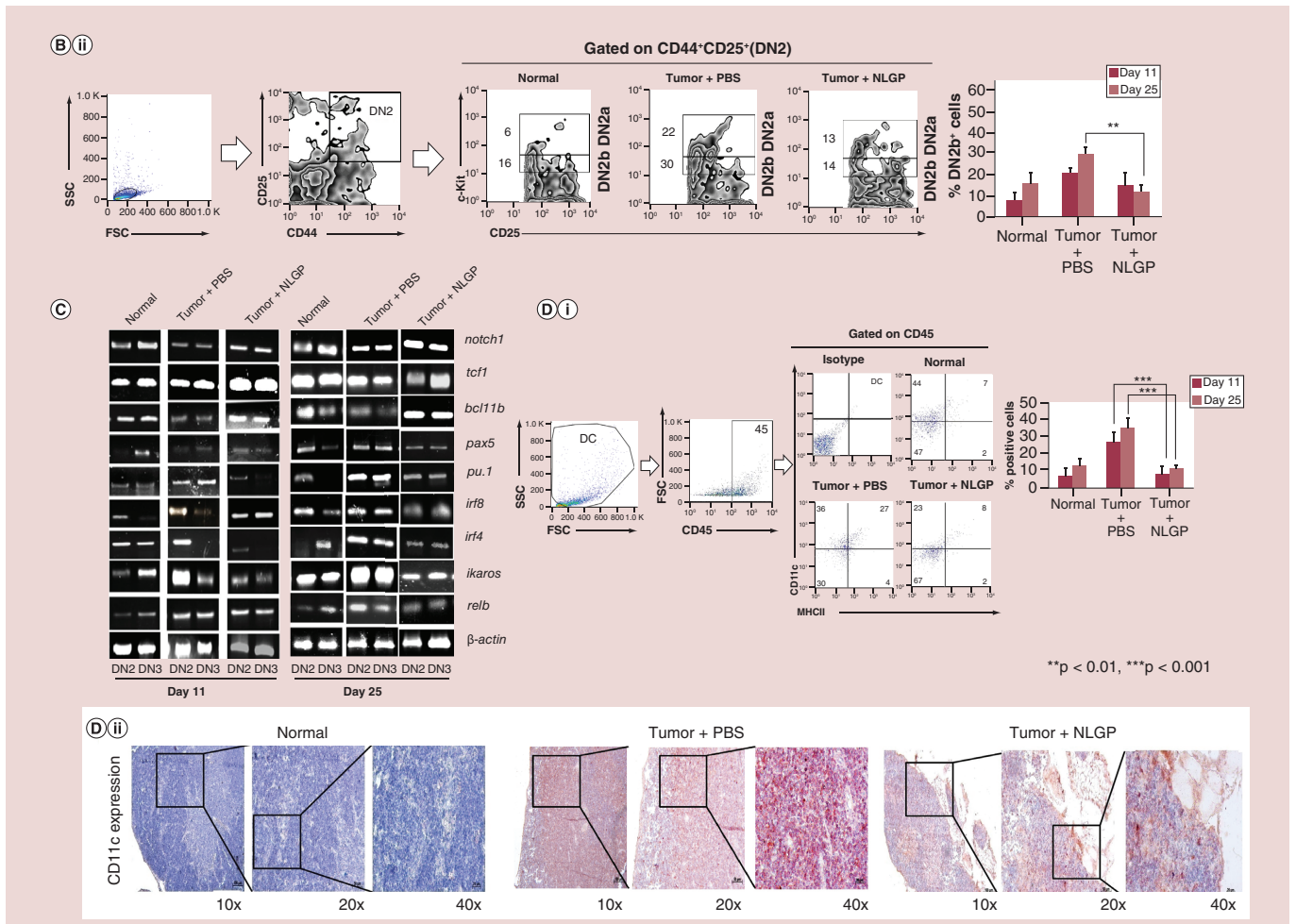


Figure 3. Neem leaf glycoprotein promotes T cell commitment by differentially regulating Notch1 and Ikaros signaling (cont.). (A) Flow-cytometric analysis of thymic T cells based on CD25 and CD44 representing DN1 to DN4 T cells of normal, tumor + PBS and tumor + NLGP mice cohorts. Bar diagrammatic representation shows mean \pm SEM of positive percentage of DN1 (CD25⁺CD44⁺), DN2 (CD25⁺CD44⁺), DN3 (CD25⁺CD44⁻) and DN4 (CD25⁻CD44⁻) T cells from above mentioned mice groups. (Bi) Immunofluorescence staining with CD25-PE and CD44-FITC was performed in thymuses from normal, tumor + PBS and tumor + NLGP hosts. Representative merged figure of stained tissues show the co-localization of CD25 and CD44 and dotted circles indicate the CD44⁺CD25⁺ localized regions. Representative 2D intensity histogram shows colocalization of CD25 and CD44; Manders' co-efficient represents the intensity and index of colocalization. Value close to 1 indicates reliable colocalization, (n = 4 in each case). (Bii) Flow-cytometric representation of thymic T cells with CD25, CD44 and c-Kit staining represent the percentage of DN2a (CD25⁺CD44⁺c-Kit^{high}) and DN2b (CD25⁺CD44⁺c-Kit^{low}) cells from normal, tumor + PBS and tumor + NLGP mice groups (mean \pm SEM), n = 4, p-values are indicated in corresponding figures. (C) Thymic T cells were flow-cytometrically sorted for CD25⁺CD44⁺ as DN2 and DN3 respectively from normal, tumor + PBS and tumor + NLGP mice cohorts on day 11 and 25 after tumor inoculation. Using isolated mRNAs, different gene expressions were checked by RT-PCR, keeping β -actin as a loading control. *notch1* and *tcf1*, for T cell lineage; *pax5* for B cell lineage and *pu.1*, *ikaros*, *irf8*, *irf4* and *relb* for myeloid lineage commitment were checked. (Di) Thymic cells were stained with CD45, CD11c and MHCII. Dot plot representation of CD45⁺CD11c⁺MHCII⁺ reveals the number of total dendritic cells. Bar diagram represents mean \pm SEM of percent positive cells of CD45⁺CD11c⁺MHCII⁺ population assessed by flow-cytometry from above mentioned mice groups, (n = 3 in each groups); ***p < 0.001. (Dii) CD11c rich regions were identified immunohistochemically in thymus from normal, tumor + PBS and tumor + NLGP mice cohorts and shown in 10x, 20x and 40x magnifications. NLGP: Neem leaf glycoprotein; PBS: Phosphate-buffered saline.

Supplementary Figures 2, 3 & 4). As systemic inflammatory cytokine cascade contributes to acute thymic involution resulting in impaired thymopoiesis, expressions of *il-7*, *il-10*, *il-6* and *il-2* were checked by RT-PCR from 6 and 8 month aged elderly mice with or without NLGP treatment (Figure 5Ci & Cii). Prominent increase in *il-10*, *il-10r* and decrease in *il-7*, *il-7r* was observed in thymus from elderly tumor host and NLGP therapy reverses the situation by downregulating *il-10* and upregulating *il-7*.

Discussion

We have consistently reported the restriction of murine sarcoma, melanoma and carcinoma growth by NLGP immunotherapy, which coordinately results in activation of CD8⁺ T cells, dendritic cells, NK/NK-T cells, generation of memory cells, vascular normalization and reduction in metastasis [11,12,24,38]. Although the origin and growth rate of these tumors are different in many aspects, efficacy of NLGP in restriction of tumor growth was observed in all these models. Sarcoma, a connective tissue-originated tumor, grows faster than carcinoma, an epithelial cell-originated tumor, whereas the aggressive nature of melanoma form of skin cancer promotes metastasis faster than these two. These subcutaneous primary tumor models are ectopic in nature in our experimental settings. Overall data indicate that the growth rate of these tumors is different and tumor-induced thymic atrophy is also quantitatively different but same in qualitative measure in all types of tumors [20,39]. Moreover, it is also important to note that number of tumor cells inoculated to induce subcutaneous primary tumors were different (melanoma: 2×10^5 cells/ml; sarcoma: 1×10^6 cells/ml; and carcinoma: 2×10^5 cells/ml) but with progression of primary tumor growth overall immunosuppression was observed in all three models with difference in their extent. Despite the difference in origin and nature of tumor, the immunomodulatory effect of NLGP is closely identical on restriction of the tumor growth, along with normalization of thymic involution in all scenarios.

NLGP is a glycoprotein consisting of 33% of glyco part, which includes glucose, galactose and arabinose. The remaining portion is protein. Both carbohydrate and protein parts are essential for NLGP's biological action. Initial data suggest that in nondenatured PAGE it appears as a single protein, but in SDS-PAGE three components are observed. However, this preliminary observation needs further validation. A study using mass spectrometry and MALDI-TOF is undergoing to decipher its complete structure [Das *et al.*, Unpublished Data]. Earlier *in vitro* and *in vivo* studies suggested its non-toxic [40] nature and, based on our previous study, we have used 25 μ g/mice (*in vivo*) and 1.5 μ g/ml (*in vitro*) as optimum dose for NLGP therapy [5]. We have checked the bioavailability of NLGP in blood and urine using ELISA and fluorometric assay (data not shown), suggesting availability of the NLGP in

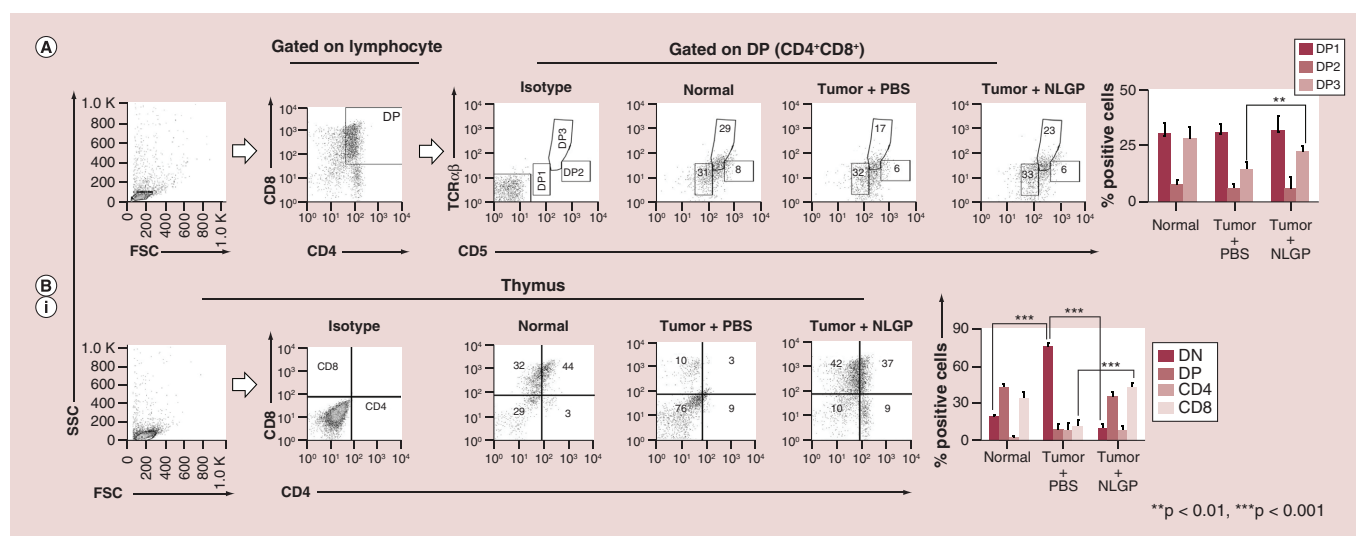


Figure 4. Double positive to CD8⁺ single positive T cell differentiation selectively promoted by neem leaf glycoprotein in tumor hosts. (A) Thymic T cells were analyzed for CD4 and CD8 and CD4⁺CD8⁺ (DP) cells were identified. Further analysis was performed by CD5 and TCR $\alpha\beta$ in normal, tumor + PBS and tumor + NLGP treated cohorts. Dot plot analysis represents DP1 (CD5^{low}TCR $\alpha\beta$ ^{low}), DP2 (CD5^{high}TCR $\alpha\beta$ ^{int}) and DP3 (CD5^{int}TCR $\alpha\beta$ ^{high}) thymic T cells. Bar diagram represent mean \pm SEM of positive percentage of DP1, DP2 and DP3 cells as identified by mentioned markers, (n = 4 in each group) **p < 0.01. (B) Thymic T cells were analyzed by CD4 and CD8 staining. Dot plot representation shows CD4⁺CD8⁻ (DN), CD4⁺CD8⁺ (DP), CD4⁺SP and CD8⁺SP T cells of thymus from normal, tumor + PBS and tumor + NLGP hosts along with bar diagrammatic representation of mean \pm SEM of positive percentage of DN, DP, SPCD4⁺ and SPCD8⁺ cells (Bi). Dot plot representation shows CD4⁺SP and CD8⁺SP T cells of blood (Bii) from all three groups, which are mentioned along with mean \pm SEM of positive percentage of SPCD4⁺ and SPCD8⁺ cells. Dot plot representation shows CD4⁺SP and CD8⁺SP T cells of lymph node (Biii) from above mentioned groups along with bar diagrammatic representation of mean \pm SEM of positive percentage of SPCD4⁺ and SPCD8⁺ cells. Dot plot representation shows CD4⁺SP and CD8⁺SP T cells of spleen (Biv) from normal, tumor + PBS and tumor + NLGP hosts. Bar diagrammatic representation of mean \pm SEM of positive percentage of SPCD4⁺ and SPCD8⁺ cells from above mentioned mice groups (n = 4 in each group). p-values are indicated in corresponding figures. DP: Double positive; NLGP: Neem leaf glycoprotein; PBS: Phosphate-buffered saline; SP: Single positive.

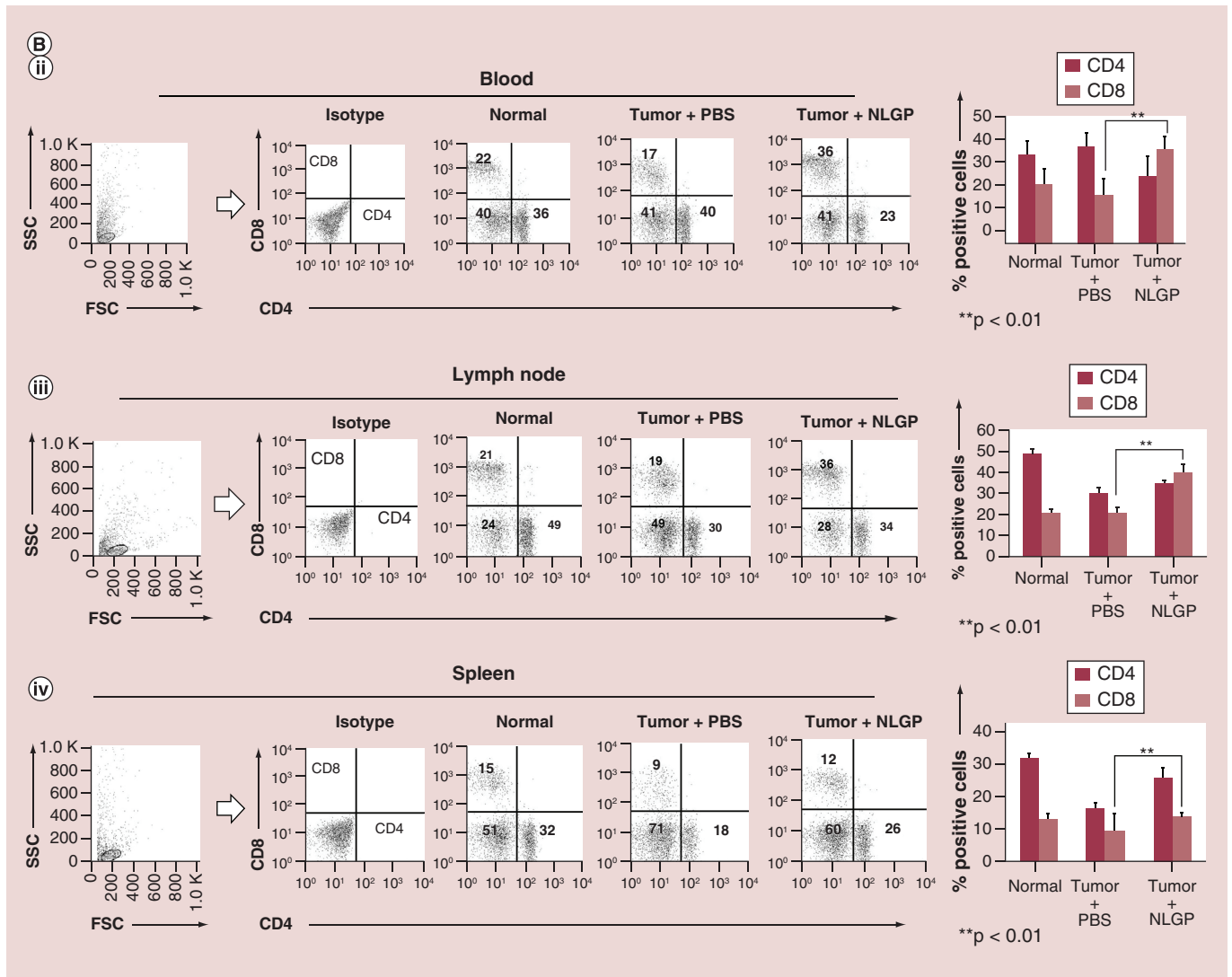


Figure 4. Double positive to CD8⁺ single positive T cell differentiation selectively promoted by neem leaf glycoprotein in tumor hosts (cont.). (A) Thymic T cells were analyzed for CD4 and CD8 and CD4⁺CD8⁺ (DP) cells were identified. Further analysis was performed by CD5 and TCR $\alpha\beta$ in normal, tumor + PBS and tumor + NLGP treated cohorts. Dot plot analysis represents DP1 (CD5^{low}TCR $\alpha\beta$ ^{low}), DP2 (CD5^{high}TCR $\alpha\beta$ ^{int}) and DP3 (CD5^{int}TCR $\alpha\beta$ ^{high}) thymic T cells. Bar diagram represent mean \pm SEM of positive percentage of DP1, DP2 and DP3 cells as identified by mentioned markers, (n = 4 in each group) **p < 0.01. (Bi) Thymic T cells were analyzed by CD4 and CD8 staining. Dot plot representation shows CD4⁻CD8⁻ (DN), CD4⁺CD8⁺ (DP), CD4⁺SP and CD8⁺SP T cells of thymus from normal, tumor + PBS and tumor + NLGP hosts along with bar diagrammatic representation of mean \pm SEM of positive percentage of DN, DP, SPCD4⁺ and SPCD8⁺ cells (Bi). Dot plot representation shows CD4⁺SP and CD8⁺SP T cells of blood (Bii) from all three groups, which are mentioned along with mean \pm SEM of positive percentage of SPCD4⁺ and SPCD8⁺ cells. Dot plot representation shows CD4⁺SP and CD8⁺SP T cells of lymph node (Biii) from above mentioned groups along with bar diagrammatic representation of mean \pm SEM of positive percentage of SPCD4⁺ and SPCD8⁺ cells. Dot plot representation shows CD4⁺SP and CD8⁺SP T cells of spleen (Biv) from normal, tumor + PBS and tumor + NLGP hosts. Bar diagrammatic representation of mean \pm SEM of positive percentage of SPCD4⁺ and SPCD8⁺ cells from above mentioned mice groups (n = 4 in each group). p-values are indicated in corresponding figures. DP: Double positive; NLGP: Neem leaf glycoprotein; PBS: Phosphate-buffered saline; SP: Single positive.

the system till 7 days. In our attempt to purify NLGP through its binding with ConA (as NLGP is a glycoprotein) and its further analysis by HPLC, we found one major component, comprising 90% of the total NLGP. Moreover, our initial *in vitro* and *in vivo* studies suggest this fraction is an effective one.

We have observed that three-times (once a week) longitudinal NLGP treatment in tumor-bearing mice reverses tumor-induced thymic alterations, in other words, thymic size, weight and cell numbers get normalized significantly. Observed antitumor functions are primarily by modulating CD8⁺ T cells, as NLGP-immunotherapy increases this

cell type and systemic depletion of CD8⁺ T cells abolished all above-mentioned features along with the NLGP-mediated tumor restriction. CD8⁺ T cells are primarily generated and educated in thymus, although this organ is believed to become atrophied after puberty. Recent data suggest that extraneous stimuli, including inflammation, hormone or cytokine therapy can reinvigorate thymopoiesis [41]. In this line, De la Rosa *et al.* mentioned that naive CD4⁺ T cells increase in HIV-infected individuals after antiretroviral therapy, which strongly support thymic T cell rejuvenation [42]. Recent research also suggests an upregulation of systemic naive Treg cells in cancer-bearing hosts [4]. Given this cumulative information, we were interested to examine whether NLGP-immunotherapy can promote thymic CD8⁺ T cell rejuvenation in the context of cancer. We also look at the thymic alterations in aged

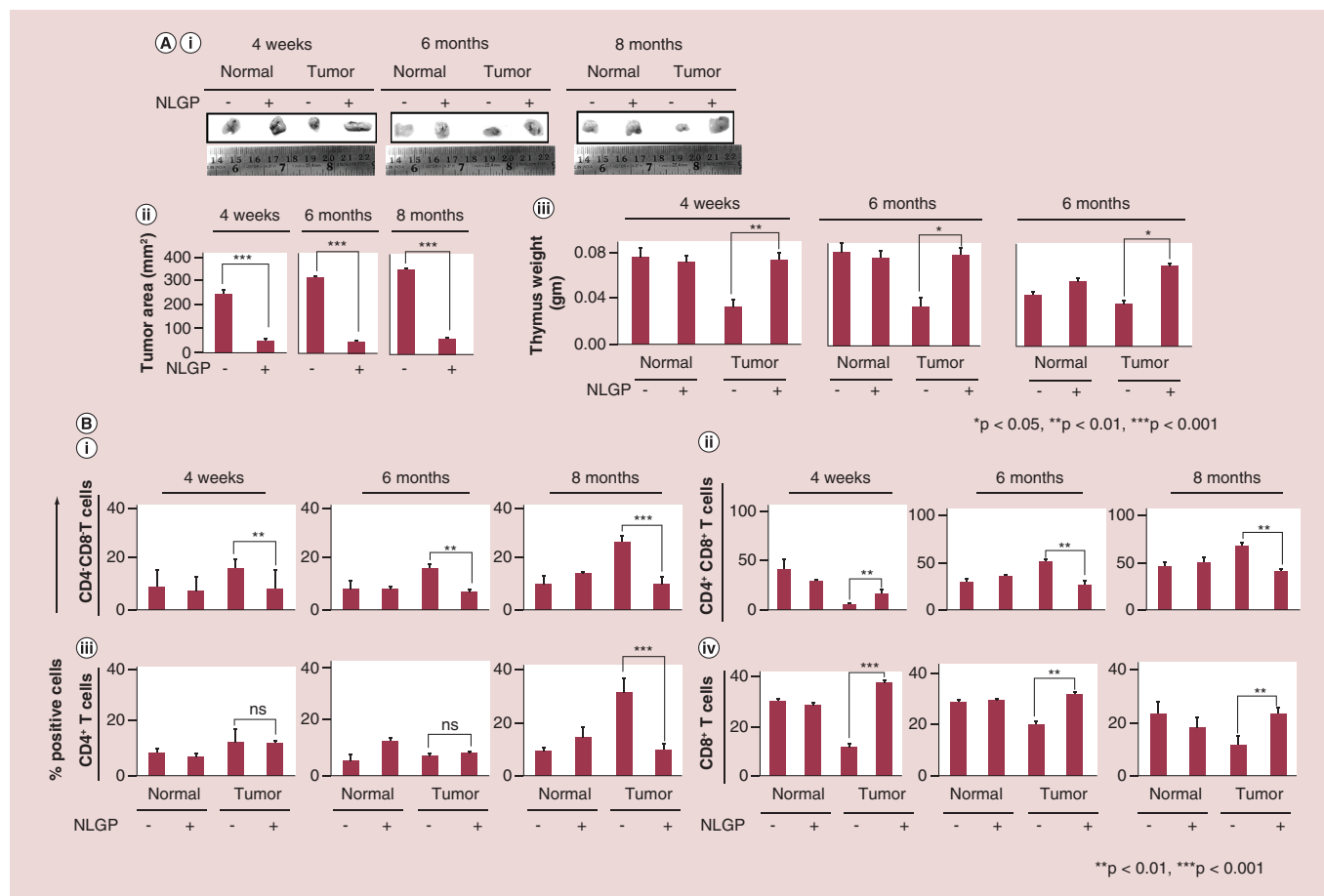


Figure 5. Neem leaf glycoprotein normalizes age associated tumor-induced thymic involution. (Ai) Representative figures from thymuses of normal + PBS, normal + NLGP, tumor + PBS and tumor + NLGP mice cohorts from three different age groups (4 weeks, 6 months and 8 months), n = 6 in each case. **(Aii)** Bar diagrammatic representation of mean ± SEM of tumor area (mm²) of four mentioned mice cohorts of three different ages (4 weeks, 6 months and 8 months) on day 11 and 25 (n = 6, in each case). **(Aiii)** Bar diagrammatic representation of thymic weight (gm) of normal + PBS, normal + NLGP, tumor + PBS and tumor + NLGP mice cohorts of 3 different ages (4 weeks, 6 months and 8 months) on day 11 and 25 (n = 6, in each case). Bar diagrammatic representation of positive percentage of **(Bi)** CD4⁺CD8⁺ (DN), **(Bii)** CD4⁺CD8⁺ (DP), **(Biii)** CD4⁺SP and **(Biv)** CD8⁺SP from normal + PBS, normal + NLGP, tumor + PBS and tumor + NLGP host (4 weeks, 6 months and 8 months) (mean ± SEM), n = 4, **p < 0.01, ***p < 0.001, ns = not significant. Dot plot representation of this flow-cytometric analysis is given in Supplementary Figure 1. **(Bv)** Splenic, **(Bvi)** blood and **(Bvii)** lymph node derived T cells harvested from normal + PBS, normal + NLGP, tumor + PBS and tumor + NLGP mice cohorts from three different age groups (4 weeks, 6 months and 8 months) were analyzed flow-cytometrically. Dot plot representation of this flow-cytometric analysis is given in Supplementary Figure 2, 3 and 4. Bar diagram represents mean ± SEM of positive percentage of CD4⁺SP and CD8⁺SP cells from mentioned mice groups; (n = 4 in each group), *p < 0.05, **p < 0.01. From total thymic mRNA, obtained from 6 and 8 months, normal and tumor hosts with or without NLGP treatment, cytokine profile was assessed by RT-PCR, keeping β-actin as a loading control. Expression of cytokines like *il-2*, *il-6*, *il-7*, *il-7r*, *il-10*, *il-10r* and *il-15* were studied by RT-PCR. **(Ci)** Representative gene expression patterns are shown in left panel, along with **(Cii)** bar diagram of mean ± SEM of from normal + PBS, normal + NLGP, tumor + PBS and tumor + NLGP hosts, (n = 4 in each group, p-values are mentioned in respective figures). NLGP: Neem leaf glycoprotein; PBS: Phosphate-buffered saline; SP: Single positive.

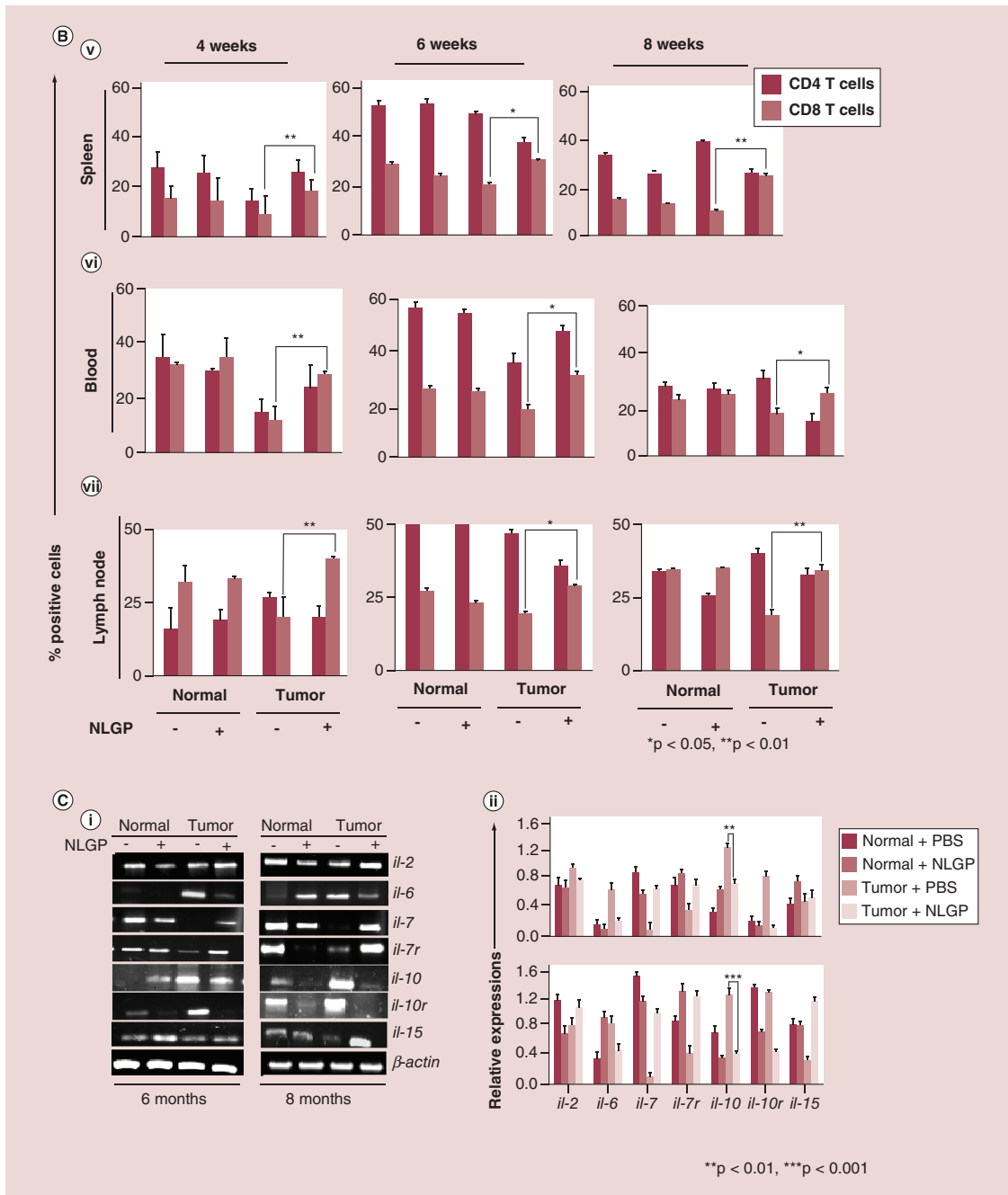


Figure 5. Neem leaf glycoprotein normalizes age associated tumor-induced thymic involution (cont.). **(Ai)** Representative figures from thymuses of normal + PBS, normal + NLGP, tumor + PBS and tumor + NLGP mice cohorts from three different age groups (4 weeks, 6 months and 8 months), n = 6 in each case. **(Aii)** Bar diagrammatic representation of mean \pm SEM of tumor area (mm²) of four mentioned mice cohorts of three different ages (4 weeks, 6 months and 8 months) on day 11 and 25 (n = 6, in each case). **(Aiii)** Bar diagrammatic representation of thymic weight (gm) of normal + PBS, normal + NLGP, tumor + PBS and tumor + NLGP mice cohorts of 3 different ages (4 weeks, 6 months and 8 months) on day 11 and 25 (n = 6, in each case). Bar diagrammatic representation of positive percentage of **(Bi)** CD4⁺CD8⁻(DN), **(Bii)** CD4⁺CD8⁺(DP), **(Biii)** CD4⁺SP and **(Biv)** CD8⁺SP from normal + PBS, normal + NLGP, tumor + PBS and tumor + NLGP host (4 weeks, 6 months and 8 months) (mean \pm SEM), n = 4, **p < 0.01, ***p < 0.001, ns = not significant. Dot plot representation of this flow-cytometric analysis is given in Supplementary Figure 1. **(Bv)** Splenic, **(Bvi)** blood and **(Bvii)** lymph node derived T cells harvested from normal + PBS, normal + NLGP, tumor + PBS and tumor + NLGP mice cohorts from three different age groups (4 weeks, 6 months and 8 months) were analyzed flow-cytometrically. Dot plot representation of this flow-cytometric analysis is given in Supplementary Figure 2, 3 and 4. Bar diagram represents mean \pm SEM of positive percentage of CD4⁺SP and CD8⁺SP cells from mentioned mice groups; (n = 4 in each group), *p < 0.05, **p < 0.01. From total thymic mRNA, obtained from 6 and 8 months, normal and tumor hosts with or without NLGP treatment, cytokine profile was assessed by RT-PCR, keeping β -actin as a loading control. Expression of cytokines like *il-2*, *il-6*, *il-7*, *il-7r*, *il-10*, *il-10r* and *il-15* were studied by RT-PCR. **(Ci)** Representative gene expression patterns are shown in left panel, along with **(Cii)** bar diagram of mean \pm SEM of from normal + PBS, normal + NLGP, tumor + PBS and tumor + NLGP hosts, (n = 4 in each group, p-values are mentioned in respective figures). NLGP: Neem leaf glycoprotein; PBS: Phosphate-buffered saline; SP: Single positive.

tumor-bearing mice, as both progressive tumorigenesis and aging are associated with thymic atrophy and affect T cell differentiation and maturation that reduces thymic T cell efflux in both mice and human.

Tumor-induced thymic atrophy results in disruption in thymic architecture, where cortex–medulla ratio gets altered, adipose tissue gets infiltrated and perivascular space gets increased, but NLGP therapy reduces perivascular spaces and normalizes cortex–medulla ratio. With aging or tumor progression these collateral alterations of intrathymic microenvironment prevents proper T cell development by targeting symbiotic interaction between thymic microenvironment and developing T cells, which depends on many factors like transcription factors, cytokines, chemokines etc. We observed a significant downregulation in *il-7* (required for T cell survivability) and *ccl19/ccl21* (maintain pro-T cell migration from cortex to sub capsular region) along with a significant upregulation of IL-10 in thymus as a major consequence of tumor progression. IL-7 is the most important gc-cytokines with a profound effect on thymopoiesis, as it regulates survivability of beta-selected DN3 thymocytes [43, 44]. Interestingly, an upregulation of thymic IL-7 was observed in NLGP treated tumor bearing mice, which may reduce the tumor-induced blockage at DN3 stage and help survivability of pro-T cells [45].

Another unique feature required for proper thymopoiesis is the highly choreographed intrathymic migration of thymocytes regulated by combination of chemokine receptor signaling and environmental cues [46]. Progressive tumor significantly downregulates the expression of chemokines, CCL19 and CCL21, both are required for CCR7-regulated intrathymic migration of DN2 cells, whereas NLGP administration normalizes *ccr7*, *ccl21* and *ccl19* expression, which may promote the migration of DN2 population toward cortex to sub-capsular region through cortico-medullary junction for further maturation of T cells. Interestingly, it was found that NLGP immunotherapy normalizes tumor induced thymic atrophy with correction in DN2–DN3 transition and also DN3–DN4 transition. During thymopoiesis (DN) pro-T cells with multi-lineage potential progress through different maturation steps: DN1 (CD25⁻CD44⁺), DN2 (CD25⁺CD44⁺), DN3 (CD25⁺CD44⁻) and DN4 (CD25⁻CD44⁻); then DP (CD4⁺CD8⁺) and SP (CD4⁺ or CD8⁺) thymocytes under the direct control of several transcription factors [47]. Progressive tumor imparted various mechanisms to target developing thymocytes. In a recent study, we have observed a significant increase in intrathymic IL-10, which downregulates Notch1 and its downstream target CCR7 to co-ordinately disturb DN-T cell migration and its interaction with thymic Keratin5⁺ stromal cells to prevent DN2–DN3 transition [20]. Stromal cells plays crucial and decisive role in thymic T cell maturation process and if stromal cells are removed from the system, T cell differentiation process gets hampered [48–50]. As *in vitro* T cell study by OP9-DL-1 system is not possible in our Institute due to nonavailability of the resources, in a separate study, we showed that tumor-related factors cause disturbed lymphostromal interaction and block proper T cell maturation [20]. Tumor-induced increase in IL-10-rich Keratin5⁺ stromal cells interact with IL-10R⁺DN2-T cells and perturbed T cell maturation [20]. In the present study, our results suggest NLGP therapy increases CCR7 expression in DN2 cells as well as enhance intrathymic expression of CCL19 and CCL21 (ligand of CCR7 and secreted from thymic stromal cells); both these events might co-operatively facilitate migration of DN2 cells from cortex to subcapsular region. Based on these results, it is speculated that NLGP's role on proper T cell differentiation might be by suppressing IL-10, which consequently promotes optimal interaction between thymic stromal cells and T cells.

NLGP treatment increases DN4 population in tumor host by regulating IL-10 and ameliorates tumor-induced arrest of DN2, specifically DN2–DN3 transition. Given the increase in DN3 and DN4 population under NLGP therapy, we have studied whether NLGP can promote their proliferation by analyzing Ki67 and *in vivo* BrdU staining, but the effect of NLGP was found to be minimal and, therefore, we have concluded that NLGP rescues tumor-induced arrest in early DN2 to DN3 transition without affecting its proliferation (Figure 6).

Tumor-induced upregulated intrathymic IL-10 arrests DN2 particularly at the thymic cortico–medullary junction, which was normalized with NLGP by rescuing IL-10-mediated suppressed Notch1 signaling. As T cell lymphopoiesis and lineage commitment are regulated by different transcription factors, here, we found that NLGP treatment upregulates *notch1*, which may license T cell lineage commitment. In tumor-bearing host, besides upregulation of notch1, NLGP downregulates tumor-induced *ikaros*, *irf8* and *pu.1* expression, which co-ordinately block the dedifferentiation of DCs from DN2 pro-T cells. On the other hand, *bcl11b* expressions, downstream regulator of notch1 [51, 52], get sustained by NLGP treatment and help lymphopoiesis toward T cell lineage commitment. Thymic DCs play a significant role in establishing self-tolerance through their ability to present self-antigens to developing T cells in the thymus by negative selection [53]. DCs also play an important role in inducing antigen-specific immunity by presenting antigens to naive T cells and differentiating the antigen specific T cells into effector cells [54]. Tumor induced thymic atrophy promotes DN2 to thymic DC generation by upregulating Ikaros/IRF8

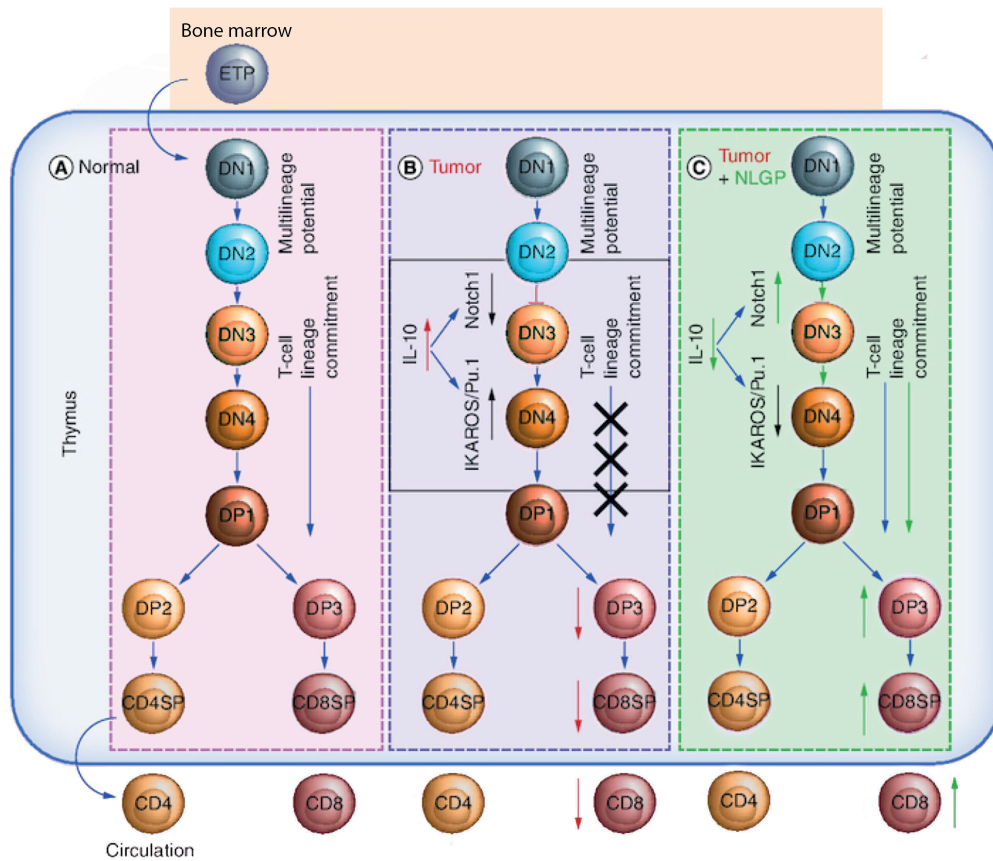


Figure 6. Mechanism of neem leaf glycoprotein mediated T cell differentiation in murine model. (A) In normal host, during thymopoiesis bone marrow derived early T cell progenitor (ETPs) enters into the thymus. These DN (CD4⁺ CD8⁻) pro-T cells with multilineage potential progress through different maturation steps: DN1, DN2, DN3 and DN4; then DP (CD4⁺ CD8⁺) and SP (CD4⁺ or CD8⁺) thymocytes, under the direct control of several transcription factors. From thymus these mature CD4 and CD8 SP thymocytes are released into the circulation. **(B)** In tumor host, in T cell developmental program, bone marrow derived early progenitor cells (ETPs) first enter into the thymus, then these DN (CD4⁺ CD8⁻) pro-T cells differentiate through different maturation steps: first step is DN1–DN2 differentiation. However, DN2–DN3, this commitment step gets arrested. Tumor induced increase of intrathymic IL-10 promotes downregulation of Notch1 along with upregulation of Ikaros and Pu.1, which results DN2 to DC differentiation instead of T cell lineage commitment. So at the end of the differentiation less number of CD8 SP thymocytes are released into the circulation. **(C)** In NLGP treated tumor cohort during thymopoiesis bone marrow derived early progenitor cells (ETPs) when enter into the thymus, they differentiate through different maturation steps: DN1, DN2, DN3, DN4 and then DP to SP. Longitudinal NLGP treatment normalizes intrathymic IL-10 and upregulates Notch1, which results T cell lineage commitment. NLGP therapy downregulates Ikaros and Pu.1 expression and normalizes DN2 to T cell lineage differentiation following release of more CD8⁺ SP T cells in circulation which restricts tumor growth. DC: Dendritic cell; DP: Double positive; ETP: Early T cell progenitor; NLGP: Neem leaf glycoprotein; SP: Single positive.

signaling instead of T cell differentiation. On the other hand, NLGP-treated tumor hosts show significant decrease in DC population (CD45⁺ MHCII⁺ CD11c⁺) from 28% to 8% on average. So it can be concluded that decrease in DCs following NLGP therapy actually implies normalization of T cell maturation and an increase in T cell pool. Although, it is known that DCs are responsible for negative selection in the thymus [55–57], our preliminary study suggests, these DN2-transformed DCs might help in Treg generation in tumor-bearing mice. However, further detailed study is required to conclude such observation. Here, NLGP treatment decreases DCs, which is beneficial because reduction in DCs implies increase in T cell generation and normalizes T cell maturation process. Understanding the detailed mechanism is the subject of our future study.

Given the influence of NLGP on T cell differentiation, next we checked intrathymic DP population in NLGP treated tumor host. DP1 to DP3 transition is another check point during intrathymic T cell differentiation, which

gets targeted by thymic atrophy, resulting production of immature T cell population [58]. In contrast, NLGP therapy generates increased proportion of DP3 (CD5^{int}TCR $\alpha\beta$ ^{high}) population specifically. As DP3 differentiates into CD8⁺ T cells [59], we further checked CD4⁺ and CD8⁺ T cells in secondary lymphoid organs and circulation. In agreement with our previous report that NLGP activates CD8⁺ T cells [5], here, we found significant influence of NLGP in increasing CD8⁺ T cells in atrophied thymus and other lymphoid organs compared with tumor hosts having no NLGP treatment. We also checked expression of ROR γ t, as it is important for survivability of DP thymocytes and during normal thymopoiesis its expression gets upregulated in CD4⁺CD8⁺ DP population [22,60]. In our model, we found less expression of ROR γ t in tumor cohort, which may be due to higher apoptotic rate of developing DP thymocytes in tumor [61]. However, in NLGP cohort we did not find any significant changes, moreover, there are a modest increase in DP thymocytes in NLGP cohort. Therefore, the little decrease in ROR γ t expression in DP thymocytes under NLGP treatment may clue the generation of more mature SP thymocytes (data not shown). However, these are only the initial observations and thus limits the inclusion of these data in the present manuscript; further study is required to confirm the role of NLGP on ROR γ t and thymocytes development. We have also studied the NLGP's effect on tumor recurrence after surgical removal of tumor (as discussed in Ghosh *et al.* [62]). The effect of NLGP is more prominent in reversal of thymic involution after surgical removal of tumor and tumor recurrence was prevented significantly in NLGP treated group. Moreover, effect of tumor restriction on immune parameters under influence of NLGP is found to be very prominent [63].

Therefore, our cumulative results suggest that NLGP immunotherapy educates the whole immune system in such a way that thymic alterations get restored with reduction of tumor growth. In the context of tumor, when we checked tumor-induced thymic atrophy and we found that tumor-induced thymic atrophy is a very common feature in cancer as we recently reported [20]. In this study, we have included two different types of tumor models of sarcoma, in other words (slow growing) and melanoma (aggressive) to test the efficacy of NLGP-therapy. Our results suggest a more rapid decrease in thymic volume in aggressive melanoma in comparison to relatively slow-growing sarcoma tumor model. C57BL/6 mice (used for melanoma) is inbred mice strain, which did not represent the heterogeneity in human population. On the other hand, Swiss mice (used for sarcoma) is outbred strain and represents more accurately human population. In respect to the effect of NLGP on these tumors and thymic atrophy, we always found the qualitative improvement of immune response in all tumor models and CD8⁺ T cell mediated restriction of primary tumor growth [5,7]. From this current work and previously published works [5,7,24], it can be stated that irrespective of tumor type and mice strain NLGP treatment improves overall immune status and restricts tumor growth by CD8⁺ T cells dependent manner and also able to prevents tumor-induced thymic atrophy. Thus, the effect of NLGP immunotherapy is not very different in context of the difference in tumor etiology.

Age-associated decline of immunity plays a pivotal role in tumorigenesis, where all the components of immune system affected to lesser or greater extent by aging and tumor burden, resulting decline in immunocompetence and surveillance. Age-related thymic regression specifically reduce the rate of naive T cell output and accumulation of DP thymocytes. This is thought to contribute to the reduction in T cell diversity in older individuals that is partially responsible for an increase in susceptibility and severity of tumor progression [64]. Influence of NLGP in elderly individual shows partial normalization of thymic size with reducing tumorigenesis along with a restoration in T cell output and thymic activity. NLGP by modulating intrathymic *il-7* and *il-15* promotes normalization of DP to SP T cell maturation in 8 months old tumor host, which may increase the overall survivability. However, the extent of NLGP's effect is found to be better in young mice than aged.

Cancer and aging have both been associated with several common biological events, like thymic atrophy, severe immune alterations etc. Tumor-induced intrathymic IL-10 paralyzes thymic T cell development program by blocking thymic DN2 to DN3 transition along with a drive to DC differentiation from pro-T cells, which finally disturb proper T cell maturation and reduce efflux of T cells. Moreover, systemic depletion of CD8⁺ T cells completely abrogated NLGP's effect on tumor [12,39]. NLGP may not be affecting thymus directly, because in normal mice and also in tumor-free aged mice the effect of NLGP is minimal. Accordingly, NLGP treatment reverses thymus from its atrophy. In this context, NLGP-based immunotherapy shows significant promise to rejuvenate thymopoiesis in the direction to enrich anti-tumor CD8⁺ T cell pool in both young and adult tumor hosts. However, whether such immunotherapy could able to prevent Treg generation is beyond the scope of present investigation.

Conclusion

In conclusion, it can be stated that non-toxic immunomodulator NLGP, which is a known activator of CD8⁺ T cells, if administered in tumor-bearing host, can reverse tumor-induced alterations in thymic architecture, cellularity and volume. More importantly, NLGP by downregulating intrathymic IL-10 rescue tumor-induced blockage in DN2 to DN3 transition by reciprocally regulating Notch1/Bcl11b and Ikaros/Irf8/Pu.1 signaling. It also helps DP to SP transition specifically to DP3 transition, which ultimately supports generation of more CD8⁺ cytotoxic T cells that may ultimately ensure restriction of tumor growth. NLGP not only rectify tumor-induced thymic alterations, but also promote same in elderly tumor hosts, which definitely support its clinical significance in cancer management.

Summary points

- Neem leaf glycoprotein (NLGP) normalizes thymic involution in various murine tumor models in proportion to the restriction of tumor growth.
- Tumor-induced thymic atrophy either in young or elderly mice results improper T cell differentiation and pronounced restriction in maintenance of circulating effector CD8⁺ T cell.
- NLGP regulates intrathymic IL-10 signaling to upregulate Notch1, which is able to rescue blockade in CD25⁺CD44⁺c-Kit⁺DN2 to CD25⁺CD44⁻c-Kit⁻DN3 transition and reverses dendritic cell differentiation toward T cell maturation.
- NLGP-based immunotherapy shows significant promise to rejuvenate thymopoiesis in the direction to enrich antitumor CD8⁺ T cell pool in both young and adult tumor hosts.

Author contributions

I Guha performed conceptualization, experimental design, experimentation, data collection and analysis, validation, FlowJo analysis, statistical analysis and manuscript preparation. A Bhuniya performed experimentation, data collection, data analysis and FlowJo analysis. P Nandi performed animal experimentation and data collection. S Dasgupta performed data collection and analysis, particularly ImageJ analysis. A Sarkar performed experimentation, data collection, data analysis and manuscript editing. A Saha performed experimentation and data collection; J Das performed animal and immunohistochemical experimentation. N Ganguly performed data analysis and figure preparation. S Ghosh, T Ghosh and M Sarkar performed experimentation and data collection; S Ghosh performed data acquisition; S Majumdar performed experimental design and support, critical comments on manuscript; R Baral performed experimental design, data analysis, manuscript preparation, manuscript editing, fund acquisition and project administration; A Bose performed conceptualization, experimental design, supervision, data analysis, manuscript and figure preparation.

Acknowledgments

We acknowledge Director, Chittaranjan National Cancer Institute, Kolkata, India, for providing all the facilities necessary for the performance of these studies. We also wish to thank P Dasgupta for his critical comments on the manuscript and all members of our laboratory for their technical support to this work. Special thanks are extended to A Rakshit, Head, Animal Facilities, CNCI for providing support for animal experiments. We acknowledge S Chowdhuri for providing neem leaves, resource for NLGP preparation.

Financial & competing interests disclosure

This study was supported by Chittaranjan National Cancer Institute, Kolkata, India and Department of Science and Technology, Govt. of India (Grant No. SR/WOS-A/LS-152/2017). These funding agencies had no role in study designing, data collection and analysis, decision to publish or the preparation of this manuscript. The authors have no other relevant affiliations or financial involvement with any organization or entity with a financial interest in or financial conflict with the subject matter or materials discussed in the manuscript apart from those disclosed.

No writing assistance was utilized in the production of this manuscript.

Ethical conduct of research

The care and treatment of animals conformed to guidelines established by the Institutional Animal Care and Ethics Committee. The study was approved by Institutional Animal care and Ethics committee (Approval No. IAEC-1774/RB-4/2015/6, IAEC-1774/RB-4(Ext)/2017/5 and IAEC-1774/RB-19/2017/15).

References

Papers of special note have been highlighted as: ● of interest; ●● of considerable interest

1. Van der Jeught K, Bialkowski L, Daszkiewicz L *et al.* Targeting the tumor microenvironment to enhance antitumor immune responses. *Oncotarget* 6(3), 1359–1381 (2015).
2. Waldmann TA. Immunotherapy: past, present and future. *Nat. Med.* 9(3), 269–277 (2003).
3. Martínez SF, Franco JM, Hernandez A *et al.* Thymopoiesis in elderly human is associated with systemic inflammatory status. *Age* 31(2), 87–97 (2009).
- **Thymus, even in elderly individuals, maintains the peripheral naive T cell pool by active thymopoiesis.**
4. Laronne-Bar-On A, Zipori D, Haran-Ghera N. Increased regulatory versus effector T cell development is associated with thymus atrophy in mouse models of multiple myeloma. *J. Immunol.* 181(5), 3714–3724 (2008).
- **As thymus is the main site of Treg development, with progressive tumorigenesis Treg production get increased in thymus instead of effector T cells.**
5. Mallick A, Barik S, Goswami KK *et al.* Neem leaf glycoprotein activates CD8⁺ T cells to promote therapeutic antitumor immunity inhibiting the growth of mouse sarcoma. *PLoS ONE* 8(1), e47434 (2013).
- **As an immunomodulator neem leaf glycoprotein treatment in tumor (sarcoma) bearing mice results tumor regression by activating CD8⁺ T cells.**
6. Barik S, Banerjee S, Mallick A *et al.* Normalization of tumor microenvironment by neem leaf glycoprotein potentiates effector T cell functions and therapeutically intervenes in the growth of mouse sarcoma. *PLoS ONE* 8(6), e66501 (2013).
7. Barik S, Bhuniya A, Banerjee S *et al.* Neem leaf glycoprotein is superior than cisplatin and sunitinib malate in restricting melanoma growth by normalization of tumor microenvironment. *Int Immunopharmacol.* 17(1), 42–49 (2013).
8. Chakraborty T, Bose A, Barik S *et al.* Neem leaf glycoprotein inhibits CD4⁺CD25⁺Foxp3⁺ Tregs to restrict murine tumor growth. *Immunotherapy* 3(8), 949–969 (2013).
9. Goswami KK, Barik S, Sarkar M *et al.* Targeting STAT3 phosphorylation by neem leaf glycoprotein prevents immune evasion exerted by supraglottic laryngeal tumor induced M2 macrophages. *Mol. Immunol.* 59(2), 119–127 (2013).
10. Sarkar M, Ghosh S, Bhuniya A *et al.* Neem leaf glycoprotein prevents post-surgical sarcoma recurrence in Swiss mice by differentially regulating cytotoxic T and myeloid-derived suppressor cells. *PLoS ONE* 12(4), e0175540 (2017).
11. Roy S, Goswami S, Bose A *et al.* Neem leaf glycoprotein partially rectifies suppressed dendritic cell functions and associated T cell efficacy in patients with stage IIIB cervical cancer. *Clin. Vaccine Immunol.* 18(4), 571–579 (2011).
12. Banerjee S, Ghosh T, Barik S *et al.* Neem leaf glycoprotein prophylaxis transduces immune dependent stop signal for tumor angiogenic switch within tumor microenvironment. *PLoS ONE* 9(11), e110040 (2014).
13. Fu Y, Paul RD, Wang Y *et al.* Thymic involution and thymocyte phenotypic alterations induced by murine mammary adenocarcinomas. *J. Immunol.* 143(12), 4300–4307 (1989).
14. Adkins B, Charyulu V, Sun QL *et al.* Early block in maturation is associated with thymic involution in mammary tumor-bearing mice. *J. Immunol.* 164(11), 5635–5640 (2000).
15. Carrio R, Lopez DM. Impaired thymopoiesis occurring during the thymic involution of tumor-bearing mice is associated with a down-regulation of the antiapoptotic proteins Bcl-XL and A1. *Int. J. Mol. Med.* 23(1), 89–98 (2009).
16. Baral R, Chattopadhyay U. Neem (*Azadirachta indica*) leaf mediated immune activation causes prophylactic growth inhibition of murine Ehrlich carcinoma and B16 melanoma. *Int. Immunopharmacol.* 4(3), 355–366 (2004).
17. Baral R, Mandal I, Chattopadhyay U. Immunostimulatory neem leaf preparation act as an adjuvant to enhance the efficacy of poorly immunogenic B16 melanoma surface antigen vaccine. *Int. Immunopharmacol.* 5(7–8), 1343–1352 (2005).
18. Chakraborty K, Bose A, Pal S *et al.* Neem leaf glycoprotein restores the impaired chemotactic activity of peripheral blood mononuclear cells from head and neck squamous cell carcinoma patients by maintaining CXCR3/CXCL10 balance. *Int. Immunopharmacol.* 8(2), 330–340 (2008).
19. Goswami S, Bose A, Sarkar K *et al.* Neem leaf glycoprotein matures myeloid derived dendritic cells and optimizes antitumor T cell functions. *Vaccine* 28(5), 1241–1252 (2010).
20. Guha I, Bhuniya A, Shukla D *et al.* Tumor arrests DN2b to DN3a pro-T cell transition and promotes its conversion to thymic dendritic cells by reciprocally regulating Notch1 and Ikaros signalling. *Front. Immunol.* 11, 898 (2020).
21. Bose A, Barik S, Banerjee S *et al.* Tumor-derived vascular pericytes anergize Th cells. *J. Immunol.* 191(2), 971–981 (2013).
22. Carrio R, Torroella-Kouri M, Iragavarapu-Charyulu V *et al.* Tumor-induced thymic atrophy: alteration in interferons and Jak/Stats signaling pathways. *Int. J. Oncol.* 38(2), 547–553 (2011).
23. Carrio R, Lopez M. Insights into thymic involution in tumor-bearing mice. *Immunol. Res.* 57(1–3), 106–114 (2013).
- **During tumorigenesis thymic involution results dysregulation in T cell differentiation and accumulation of early thymocytes which trigger changes in cytokine level also and altered thymic microenvironment in tumor host induces thymic involution.**

24. Ghosh S, Sarkar M, Ghosh T *et al.* Neem leaf glycoprotein promotes dual generation of central and effector memory CD8⁺ T cells against sarcoma antigen vaccine to induce protective antitumor immunity. *Mol. Immunol.* 71, 42–53 (2016).
25. Ghosh S, Sarkar M, Ghosh T *et al.* Absence of CD4(+) T cell help generates corrupt CD8(+) effector T cells in sarcoma-bearing Swiss mice treated with NLGP vaccine. *Immunol. Lett.* 175, 31–39 (2016).
- **Neem leaf glycoprotein promotes generation of CD8⁺ T cells in tumor bearing mice with the help of CD4⁺ T cells.**
26. Elmore SA. Enhanced histopathology of the thymus. *Toxicol. Pathol.* 34(5), 656–665 (2006).
27. Carding SR, Hayday AC, Bottomly K. Cytokines in T cell development. *Immunol. Today* 12(7), 239–245 (1991).
28. Ciofani M, Zúñiga-Pflücker JC. The thymus as an inductive site for T lymphopoiesis. *Annu. Rev. Cell Dev. Biol.* 23, 463–493 (2007).
29. Schwarz BA, Sambandam A, Maillard I *et al.* Selective thymus settling regulated by cytokine and chemokine receptors. *J. Immunol.* 15(4), 2008–2017 (2007).
30. Landskron G, De la Fuente M, Thuwajit P *et al.* Chronic inflammation and cytokines in the tumor microenvironment. *J. Immunol. Res.* 2014, 149185 (2014).
31. Soldevila G, Licona I, Salgado A *et al.* Impaired chemokine-induced migration during T cell development in the absence of Jak 3. *Immunology* 112(2), 191–200 (2004).
32. Ueno T, Saito F, Gray DH *et al.* CCR7 signals are essential for cortex-medulla migration of developing thymocytes. *J. Exp. Med.* 200(4), 493–505 (2004).
- **CCR7 controls migration of thymocytes in between cortex and medulla whereas CCR7 or its ligand deficient mice shows arrest of thymocytes in the cortex and dysregulation in T cell differentiation.**
33. Rothenberg EV, Moore JE. Launching the T-Lineage developmental programme. *Nat. Rev. Immunol.* 8(1), 9–21 (2008).
- **In thymus multipotent early progenitor thymocytes differentiate and committed towards T cell progenitor by the upregulation of T cell lineage genes and downregulation of non-T cell lineage specific genes.**
34. Shah D, Flicker J. An overview of the intrathymic intricacies of T cell development. *J. Immunol.* 192(9), 4017–4023 (2014).
35. Seo W, Taniuchi I. Transcriptional regulation of early T cell development in the thymus. *Eur. J. Immunol.* 46(3), 531–538 (2016).
36. Wakabayashi Y, Watanabe H, Inoue J *et al.* Bcl11b is required for differentiation and survival of alphabeta T lymphocytes. *Nat. Immunol.* 4(6), 533–539 (2003).
37. Avram D, Califano D. The multifaceted roles of Bcl11b in thymic and peripheral T cells: impact on immune diseases. *J. Immunol.* 193(5), 2059–2065 (2014).
38. Bose A, Chakraborty K, Sarkar K *et al.* Neem leaf glycoprotein induces perforin mediated tumor cell killing by T and NK cells through differential regulation of IFN γ signaling. *J. Immunother.* 32(1), 42–53 (2009).
39. Bhuniya A, Guha I, Ganguly N *et al.* NLGP attenuates murine melanoma and carcinoma metastasis by modulating cytotoxic CD8(+) T cells. *Front. Oncol.* 10, 201 (2020).
40. Mallick A, Ghosh S, Banerjee S, Majumder S *et al.* Neem leaf glycoprotein is nontoxic to physiological functions of Swiss mice and Sprague Dawley rats: histological, biochemical and immunological perspectives. *Int. Immunopharmacol.* 15(1), 73–83 (2013).
41. Majumdar S, Nandi D. Thymic atrophy: experimental studies and therapeutic interventions. *Scand. J. Immunol.* 87(1), 4–14 (2018).
42. De la Rosa R, Leal M. Thymic involvement in recovery of immunity among HIV-infected adults on highly active antiretroviral therapy. *J. Antimicrob. Chemother.* 52(2), 155–158 (2003).
43. Peschon JJ, Morrissey PJ, Grabstein KH *et al.* Early lymphocyte expansion is severely impaired in interleukin 7 receptor-deficient mice. *J. Exp. Med.* 180(5), 1955–1960 (1994).
44. Tussiwand R, Engdahl C, Gehre N *et al.* The preTCR-dependent DN3 to DP transition requires Notch signaling is improved by CXCL12 signaling and is inhibited by IL-7 signaling. *Eur. J. Immunol.* 4(11), 3371–3380 (2011).
45. Boudil A, Matei IR, Shih HY *et al.* IL-7 coordinates proliferation, differentiation and Tcr α recombination during thymocyte β -selection. *Nat. Immunol.* 16(4), 397–405 (2015).
- **In thymus, IL-7 plays an important role with coordination with preTCR and Notch1 for proliferation and differentiation of T cells during β selection.**
46. Bunting MD, Comerford I, McColl SR. Finding their niche: chemokines directing cell migration in the thymus. *Immunol. Cell Biol.* 89(2), 185–196 (2011).
47. Rothenberg EV, Ungerback J, Champhekar A. Forging T-lymphocyte identity: intersecting networks of transcriptional control. *Adv. Immunol.* 129, 109–174 (2016).
48. Takahama Y. Journey through the thymus: stromal guides for T cell development and selection. *Nat. Rev. Immunol.* 6(2), 127–135 (2006).
49. Nitta T, Suzuki H. Thymic stromal cell subsets for T cell development. *Cell. Mol. Life Sci.* 73(5), 1021–1037 (2016).
50. James KD, Jenkinson WE anderson G. T cell egress from the thymus: should I stay or should I go? *J. Leukoc. Biol.* 104(2), 275–284 (2018).

51. Tydell CC, David-Fung ES, Moore JE *et al.* Molecular dissection of prethymic progenitor entry into the T lymphocyte developmental pathway. *J. Immunol.* 179(1), 421–438 (2007).
 52. Li L, Leid M, Rothenberg EV. An early T cell lineage commitment checkpoint dependent on the transcription factor *Bcl11b*. *Science* 329(5987), 89–93 (2010).
 53. Bonasio R, Scimone ML, Schaerli P *et al.* Clonal deletion of thymocytes by circulating dendritic cells homing to the thymus. *Nat. Immunol.* 7(10), 1092–1100 (2006).
 54. Audiger C, Rahman MJ, Yun TJ *et al.* The importance of dendritic cells in maintaining immune tolerance. *J. Immunol.* 198(6), 2223–2231 (2017).
 55. Brocker T. The role of dendritic cells in T cell selection and survival. *J. Leukoc. Biol.* 66(2), 331–335 (1999).
 56. Cannarile AM, Decanis N, van Meerwijk JPM *et al.* The role of dendritic cells in selection of classical and nonclassical CD8⁺ T cells *in vivo*. *J. Immunol.* 173(8), 4799–4805 (2004).
 57. Kroger CJ, Spidale NA 1, Wang B *et al.* Thymic dendritic cell subsets display distinct efficiencies and mechanisms of intercellular MHC transfer. *J. Immunol.* 198(1), 249–256 (2017).
 58. Xing Y, Hogquist KA. T cell tolerance: central and peripheral. *Cold Spring Harb. Perspect. Biol.* 4(6), a006957 (2012).
 59. Sinclair C, Seddon B. Overlapping and asymmetric functions of TCR signaling during thymic selection of CD4 and CD8 lineages. *J. Immunol.* 192(11), 5151–5159 (2014).
 60. He YW. The role of orphan nuclear receptor in thymocyte differentiation and lymphoid organ development. *Immunol. Res.* 22(2–3), 71–82 (2000).
 61. Guo Y, MacIsaac KD 2, Chen Y *et al.* Inhibition of ROR γ T skews TCR α gene rearrangement and limits T cell repertoire diversity. *Cell Rep.* 17(12), 3206–3218 (2016).
 62. Ghosh S, Sarkar M, Ghosh T *et al.* Neem leaf glycoprotein generates superior tumor specific central memory CD8⁺ T cells than cyclophosphamide that averts post-surgery solid sarcoma recurrence. *Vaccine* 35(34), 4421–4429 (2017).
 63. Sarkar M, Ghosh S, Bhuniya A *et al.* Neem leaf glycoprotein prevents post-surgical sarcoma recurrence in Swiss mice by differentially regulating cytotoxic T and myeloid-derived suppressor cells. *PLoS ONE* 12(4), e0175540 (2017).
 64. Weng NP. Aging of the immune system: how much can the adaptive immune system adapt? *Immunity* 24(5), 495–499 (2006).
- **Aging results decline in production of naive T cells in the thymus which is known as age associated thymic atrophy, such thymic atrophy is regulated by several factors.**